The binding of activated Gα_q to phospholipase C-β exhibits anomalous affinity

Received for publication, July 31, 2017, and in revised form, August 22, 2017 Published, Papers in Press, August 24, 2017, DOI 10.1074/jbc.M117.809673

Punya Navaratnarajah[‡], **Anne Gershenson**[§], **and Elliott M. Ross**[‡1]

From the [‡]*Department of Pharmacology and Green Center for Systems Biology, University of Texas Southwestern Medical Center, Dallas, Texas 75390-9041 and the* [§]*Department of Biochemistry and Molecular Biology, University of Massachusetts, Amherst, Massachusetts 01003-9292*

Edited by Henrik G. Dohlman

Upon activation by the G_q family of Gα subunits, G$\beta\gamma$ subunits, and some Rho family GTPases, phospholipase C-β (PLC-β) isoforms hydrolyze phosphatidylinositol 4,5-bisphosphate to the second messengers inositol 1,4,5-trisphosphate and diacylglycerol. PLC-β isoforms also function as GTPase-activating proteins, potentiating G_q deactivation. To elucidate the mechanism of this mutual regulation, we measured the thermodynamics and kinetics of PLC-β3 binding to Gα_q. FRET and fluorescence correlation spectroscopy, two physically distinct methods, both yielded K_d values of about 200 nM for PLC-β3–Gα_q binding. This K_d is 50–100 times greater than the EC_{50} for Gα_q-mediated PLC-β3 activation and for the Gα_q GTPase-activating protein activity of PLC-β. The measured K_d was not altered either by the presence of phospholipid vesicles, phosphatidylinositol 4,5-bisphosphate and Ca^{2+}, or by the identity of the fluorescent labels. FRET-based kinetic measurements were also consistent with a K_d of 200 nM. We determined that PLC-β3 hysteresis, whereby PLC-β3 remains active for some time following either Gα_q–PLC-β3 dissociation or PLC-β3–potentiated Gα_q deactivation, is not sufficient to explain the observed discrepancy between EC_{50} and K_d. These results indicate that the mechanism by which Gα_q and PLC-β3 mutually regulate each other is far more complex than a simple, two-state allosteric model and instead is probably kinetically determined.

In animals, phospholipase C (PLC)[2] hydrolyzes phosphatidylinositol 4,5-bisphosphate (PIP_2) to inositol 1,4,5-trisphosphate and diacylglycerol, two important second messengers that regulate diverse cellular processes in response to multiple extracellular stimuli that act through diverse mechanisms (1). The four PLC-β family members are stimulated by the G_q family of Gα subunits, G$\beta\gamma$ subunits, and Rac GTPases, and PLC-β function is consequently central to numerous signaling pathways in all animal cells (2). PLC-β also contributes directly to the temporal dynamics of its activation because it is a GTPase-activating protein (GAP) for Gα_q and can accelerate deactivation of Gα_q–GTP >1000-fold (3).

Gα_q, G$\beta\gamma$, and Rac all bind independently to PLC-βs to cause activation, although G$\beta\gamma$ does not activate PLC-β4 (4), and only PLC-β2 is stimulated by Rac (5, 6). The activity of PLC-β3 can be simulated about 400-fold by Gα_q (7). Gα_q and G$\beta\gamma$ activate PLC-β3 synergistically, and relative activation can exceed 2000-fold (7). Despite the availability of several X-ray crystal structures of Gα_q, G$\beta\gamma$, PLC-β3, and the PLC-β3–Gα_q complex (8–13) plus considerable enzymologic studies (3, 7, 10, 12, 14–21), the details of this activation process remain unclear. Activation requires both binding of PLC-β to the surface of the membrane that contains the PIP_2 substrate and the movement of an autoinhibitory loop away from the active site (10, 22). Additional intramolecular events may also be involved. Sondek and co-workers (10, 22) suggested that Gα_q anchors PLC-β to the membrane surface and that the anionic autoinhibitory region is forced away from the active site simply by charge repulsion between this region and the membrane. Both proteins bind to distinct sites on PLC-β and could force the PLC-β against the bilayer, although the geometry of this interaction is uncertain (8, 10–12, 20, 22). In addition, Lyon *et al.* (11) pointed out that binding to Gα_q may disrupt intramolecular contacts in PLC-β that, in the absence of activator, stabilize the autoinhibitory region over the active site. The role of the C-terminal helical domain, which is essentially required for activation by Gα_q but not by G$\beta\gamma$, is not understood (8, 12, 14, 20); nor is the way that movement of the PH domain during G$\beta\gamma$ binding leads to activation (19).

At a descriptive level, Gα_q has been assumed to activate PLC-β by a simple allosteric mechanism in which Gα_q binding drives a structural isomerization of the PLC to a more active conformation or orientation with respect to the bilayer surface (2, 23). In the simplest case of allosteric activation, the EC_{50} for activating an enzyme by a ligand is equal to the equilibrium dissociation constant for ligand binding, K_d, although various mechanisms can cause deviation from this pattern (24). GTP-activated Gα_q stimulates PLC-βs with EC_{50} values of ~1–5 nM

This work was supported by National Institutes of Health Grants R01GM030355 and R21DC015744 (to E. M. R.) and R01GM060418 (to A. G.). The authors declare that they have no conflicts of interest with the contents of this article. The content is solely the responsibility of the authors and does not necessarily represent the official views of the National Institutes of Health.

This article contains supplemental Table S1 and Fig. S1.

[1] To whom correspondence should be addressed: Dept. of Pharmacology, University of Texas Southwestern Medical Center, 6001 Forest Park Rd., Dallas, TX 75390-9041. Tel.: 214-645-6134; E-mail: Elliott.Ross@UTSouthwestern.edu.

[2] The abbreviations used are: PLC, phospholipase C; PIP_2, phosphatidylinositol 4,5-bisphosphate; GAP, GTPase-activating protein; PH, pleckstrin homology; FCS, fluorescence correlation spectroscopy; GTPγS, guanosine 5′-O-[γ-thio]triphosphate; PE, phosphatidylethanolamine; PS, phosphatidylserine; m1AChR, m1 muscarinic acetylcholine receptor; PC, phosphatidylcholine; Alx, Alexa Fluor®; Cer, cerulean fluorescent protein; NTA, nitrilotriacetic acid; IP_3, inositol 1,4,5-trisphosphate.

(7, 11, 16). These values agree with the EC_{50} for the G_q GAP activity of PLC-β, the ability of PLC-β to accelerate hydrolysis of Gα$_q$-bound GTP (3, 10, 16). Therefore, we expected the K_d for PLC-β3 binding to Gα$_q$ to be in the 1–5 nM range. In fact, the first reported K_d values for Gα$_q$ and PLC-β binding were in the low nanomolar range, consistent with the EC_{50} (25), although Waldo *et al.* (10) reported a K_d for PLC-β3 binding to Gα$_q$ of about 200 nM.

To further probe the mechanism of PLC-β activation, we describe here two physically different but complementary measurements of the binding of GTPγS-activated Gα$_q$ to PLC-β3. One is based on intermolecular FRET between the two proteins, and the other is based on fluorescence correlation spectroscopy (FCS) measurements of the decrease in Gα$_q$ diffusion when it is bound to PLC-β3. Both methods yielded values for K_d of about 200 nM, which is 50–100 times greater than the EC_{50} for activation of PLC-β3 by Gα$_q$ or for acceleration by PLC-β of hydrolysis of Gα$_q$-bound GTP. The FRET assay allowed us to perform multiple controls for the validity of the determination and to show that binding affinity is relatively insensitive to minor variation in experimental conditions. This disagreement in EC_{50} and K_d is not explained by an essential activator mechanism (24) or by the simplest hysteretic models. Our data suggest that activation of PLC-β by Gα$_q$ in the low nanomolar range is not mediated by the thermodynamically most stable state but rather reflects a fast and transient interaction of the two proteins on the bilayer surface.

Results

To study the mechanism of PLC-β activation by Gα$_q$ and the G_q GAP activity of PLC-β, we measured the equilibrium binding of the two proteins and their rates of association and dissociation in comparison with their functional interactions.

Equilibrium Gα$_q$–PLC-β3 binding measured by FRET

We developed a FRET-based binding assay to measure the thermodynamics and kinetics of PLC-β3 binding to Gα$_q$. Both proteins were mutated to remove endogenous reactive cysteine residues and labeled at individual novel cysteine residues with donor or acceptor fluorophores. Several such FRET pairs were tested for energy transfer (see below). As an example, we first describe binding measured using a single Gα$_q$–PLC-β3 FRET pair in which cysteine residues introduced in place of Glu^{249} in Gα$_q$ and Gln^{871} in PLC-β3 were labeled with Alexa Fluor 488 and 594 maleimide, respectively (see "Experimental procedures"). These labeled proteins are referred to as Gα$_q$-F and PLC-β3-Q. Both proteins behave identically to wild-type, unlabeled proteins with respect to catalytic and regulatory activities (see Fig. 2). Other fluorescently labeled proteins, also checked for catalytic and regulatory activities, are described below.

When GTPγS-bound Gα$_q$-F (Gα$_q$-F–GTPγS) was mixed with PLC-β3-Q, donor fluorescence was quenched, and acceptor fluorescence was increased in parallel (Fig. 1*A*), although FRET-driven acceptor emission is only obvious at low PLC-β3-Q concentrations because it is masked by direct excitation. Binding of Gα$_q$-F to PLC-β3-Q saturated at about 50% donor quenching when increasing amounts of PLC-β3-Q were added to a fixed concentration of fully activated Gα$_q$-F–GTPγS (Fig. 1, *B* and *C*). Incomplete Gα$_q$-F activation decreased maximum quenching but did not alter affinity of binding. Donor quenching was fit to a single-site binding equation to yield the equilibrium dissociation constant, K_d. Under standard phospholipase assay conditions with buffer that includes unilamellar 1-stearoyl-2-arachidonoyl-phosphatidylethanolamine (PE)/phosphatidylserine (PS)/PIP_2 (16:4:1; 262 μM total) vesicles and 60 nM free Ca^{2+}, the K_d for binding was 160 ± 50 nM (n = 2) (Fig. 1*B*). Binding was also measured under a variety of other conditions without much change in affinity (Table 1). Without Ca^{2+}, the K_d was 242 ± 18 nM (n = 3) (Fig. 1*C*); without PIP_2 but with Ca^{2+}, the K_d was 280 ± 30 nM (supplemental Fig. S1*A*) (n = 2). Phospholipid vesicles are not required for Gα$_q$–PLC-β3 binding (supplemental Fig. S1, *B* and *C*). In 0.2% cholate, the K_d was 140 ± 30 nM (supplemental Fig. S1*B*), and without detergent or phospholipid, the K_d was 110 ± 20 nM (supplemental Fig. S1*C*). These values of K_d, all about 200 nM, are not significantly different at a level of p = 0.08 (lowest p value of 10 pairwise t tests). Hence, regardless of whether the PLC-β substrate PIP_2 or Ca^{2+} was present, the K_d for Gα$_q$ binding to PLC-β3 was ~200 nM. The concentration of the Gα$_q$-F–GTPγS FRET donor also did not alter the value of K_d over the range of 2–10 nM.

Gα$_q$ binding to PLC-β3 depends on Gα$_q$ activation. Gα$_q$-F–GDP, which does not activate PLC-β at attainable concentrations, was only 8% quenched by 4000 nM PLC-β3-Q, ~20 times the K_d for GTPγS-activated Gα$_q$-F (Fig. 1*C*; see also supplemental Fig. S1 (*B* and *C*)). Quenching of Gα$_q$-F–GDP did not saturate, but these data are consistent with a K_d of about 50 μM, about 250-fold higher than that for activated G_q. The behavior of partially activated preparations of Gα$_q$-F is also consistent with the low affinity of Gα$_q$–GDP for PLC-β. When increasing concentrations of PLC-β3-Q were added to partially activated preparations of Gα$_q$-F, quenching saturated with K_d ~200 nM, but fractional quenching was reduced approximately in proportion to the amount of Gα$_q$ that remained bound to GDP. For example, when Gα$_q$-F was only ~40% activated by GTPγS, donor quenching was ~30% at saturating PLC-β3-Q concentrations (Fig. 1*B*). Under the same conditions, when Gα$_q$-F was ~95% active, ~50% of the donor was quenched at saturating PLC-β3-Q concentrations (Fig. 1*C*).

To further verify that donor quenching measures equilibrium binding, we tested the ability of unlabeled, wild-type PLC-β3 to compete with PLC-β3-Q for Gα$_q$-F binding. Activated wild-type PLC-β3 blocked quenching of Gα$_q$-F–GTPγS by PLC-β3-Q with a K_i of 180 ± 30 nM, similar to the K_d determined for the two labeled proteins (Fig. 1*D*). In contrast, a PLC-β3 that is mutated at a Gα$_q$-binding interface, L859E, did not inhibit donor quenching (Fig. 1*D*). This mutant is not stimulated by Gα$_q$ and does not bind Gα$_q$ according to surface plasmon resonance measurements (10). PLC-β1 also inhibited PLC-β3-Q binding with a K_i of 400 nM.

By standard criteria, the data described above indicate that GTPγS-activated Gα$_q$-F binds PLC-β3-Q reversibly with an equilibrium K_d of about 200 nM, and that binding affinity is at most modestly altered by the presence of phospholipid bilayers or detergent micelles. In contrast, GTPγS-activated Gα$_q$-F stimulates the activity of PLC-β3-Q with an EC_{50} of 2–5 nM

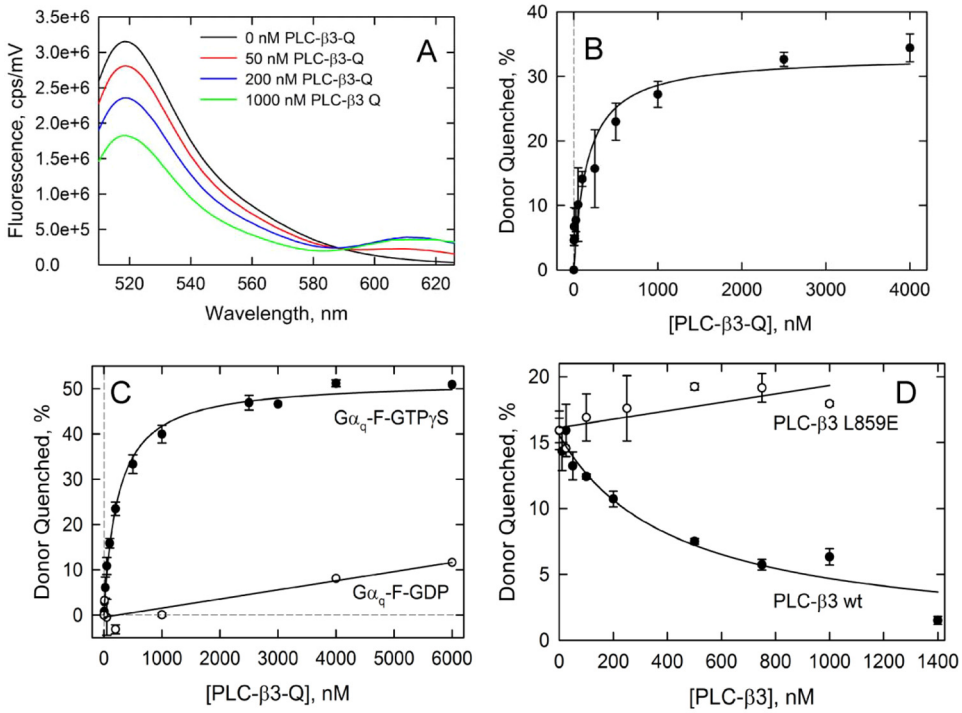

Figure 1. Equilibrium binding of PLC-β3 to Gα$_q$–GTPγS determined by FRET. *A*, donor quenching and acceptor enhancement are observed when PLC-β3-Q is added to Gα$_q$-F–GTPγS. Fluorescence spectra of 10 nM Gα$_q$-F–GTPγS alone (*black*) and with 50 nM (*red*), 200 nM (*blue*), or 1000 nM (*green*) PLC-β3-Q were obtained in the presence of PE/PS/PIP$_2$ vesicles with no added Ca^{2+}. Direct excitation of the acceptor has been subtracted. Gα$_q$-F was ~100% activated by GTPγS, and maximal quenching was 42%. *B*, binding of PLC-β3-Q to 2 nM Gα$_q$-F–GTPγS was measured according to donor quenching in the presence of PE/PS/PIP$_2$ vesicles with 60 nM Ca^{2+}. Data are the average and range of two independent experiments. The data were fit to a single-site binding equation, yielding a K_d of 160 ± 50 nM. In these experiments, Gα$_q$-F was 42% activated, and maximal donor quenching (Q_{max}) was 33 ± 2%. *C*, binding of PLC-β3-Q to 10 nM Gα$_q$-F–GTPγS (*closed circles*) was measured in the presence of PE/PS/PIP$_2$ vesicles with no added Ca^{2+}. Data are the average and range from three independent experiments. The data were fit to a single-site binding equation with K_d = 242 ± 18 nM. In these experiments, Gα$_q$-F was 95% activated, and Q_{max} = 51.8 ± 0.8%. Binding of PLC-β3-Q to Gα$_q$-F–GDP is also shown (*open circles*), with a fit to a linear function. *D*, competitive binding of PLC-β3 to Gα$_q$-F in the presence of PE/PS vesicles. Increasing concentrations of unlabeled, wild-type PLC-β3 (*closed circles*) were added to a mixture of 10 nM Gα$_q$-F and 250 nM PLC-β3-Q. The data shown are the average and range of two independent experiments. Data for wild-type PLC-β3 were fit to a model of single-site competition, yielding an IC_{50} of 430 ± 80 nM. The Gα$_q$-F was 50% activated by GTPγS, and donor quenching in the absence of inhibitor, ~16%, was consistent with the K_d determined in *B* and *C*. A third competition experiment, with Gα$_q$-F that was activated 100%, yielded ~30% donor quenching without inhibitor (data not averaged in this figure). These three competition experiments, following correction of IC_{50} values for the concentration of labeled PLC-β3 present, yielded a K_i of 180 ± 30 nM, similar to the K_d shown in *B* and *C*. The G$_q$-unresponsive mutant PLC-β3, L859E (10) (*open circles*), did not inhibit binding of 2.5 nM Gα$_q$-F–GTPγS binding to 250 nM PLC-β3-Q. Data are the average and range (*error bars*) of two independent experiments.

TABLE 1
Summary of Gα$_q$—PLC-β3 K_d measurements

Assay	Gα$_q$-GTPγS	nM	% Gα$_q$ Activated	PLC-β3	Ves./Det.	[Ca^{2+}] (nM)	K_d (nM)	Q_{max} %	Figure
FRET	Gα$_q$-F	2	42	PLC-β3-Q	PE:PS:PIP$_2$	60	160 ± 50	33 ± 2	1B
		10	95		PE:PS:PIP$_2$	0	242 ± 18	51.8 ± 0.8	1C
		2, 10	96		PE:PS	60	280 ± 30	45.9 ± 1.1	S1A
		5	92		0.2 % cholate	0	140 ± 30	40 ± 2	S1B
		2, 10	96		No Ves./Det.	0	110 ± 20	38 ± 2	S1C
		2	42	PLC-β3-wt-Alx594	PC:PE:PS	0	560 ± 110	37 ± 2	S1D
		5	92	PLC-β3-720-Alx594	PE:PS	0	210 ± 40	24.6 ± 1.1	3A
	Gα$_q$-Cer	10	72	PLC-β3-277-Alx594	PE:PS	0	270 ± 60	27 ± 2	3B
FCS	Gα$_q$-F	5	50	PLC-β3	No Ves./Det.	0	120 ± 20	N/A	4B

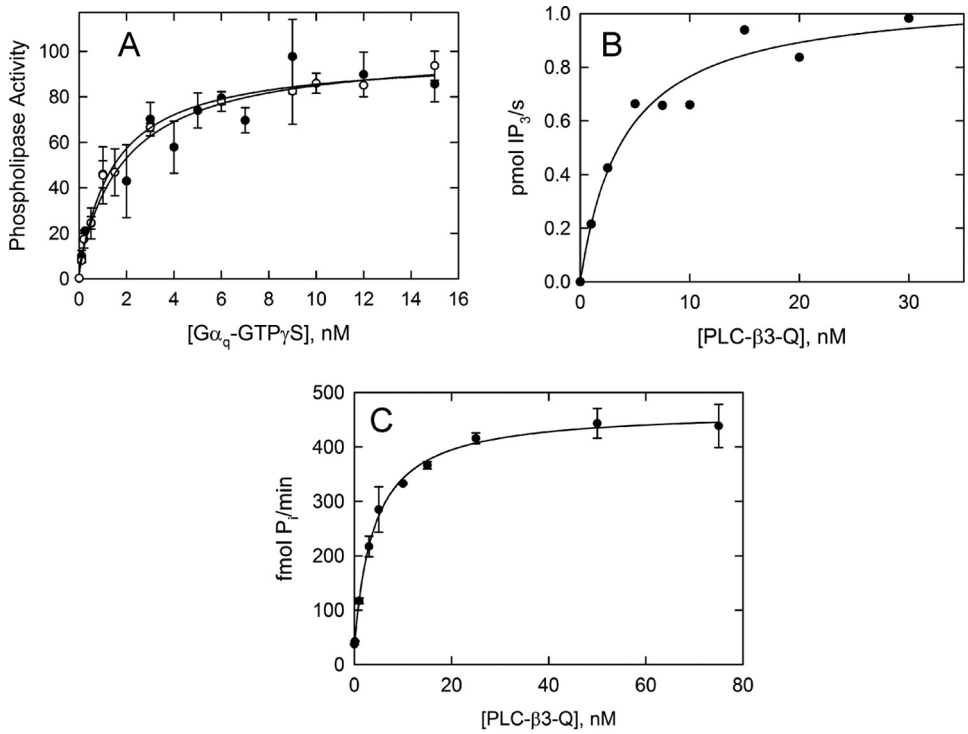

Figure 2. Fluorescently labeled Gα$_q$-F and PLC-β3-Q behave biochemically like the wild-type, unlabeled proteins. *A*, the activation of wild-type PLC-β3 by GTPγS-bound wild-type Gα$_q$ (*closed circles*) and PLC-β3-Q by Gα$_q$-F–GTPγS (*open circles*) was assayed at 60 nM free Ca^{2+}. Duplicate measurements from three independent experiments were normalized and averaged. The range of maximum reaction rates obtained was 500–4000 pmol of IP_3/min/pmol of PLC-β3. In sets of parallel experiments, EC_{50} was 2.3 ± 0.4 nM for wild-type PLC-β3 activated by wild-type Gα$_q$ (800 ± 600-fold stimulation, $n = 3$), consistent with previously reported measurements (7, 11); EC_{50} was 1.7 ± 1.1 nM for PLC-β3-Q activated by Gα$_q$-F (500 ± 300-fold stimulation, $n = 3$); EC_{50} was 4 ± 3 nM for wild-type PLC-β3 activated by Gα$_q$-F–GTPγS (220 ± 80-fold stimulation, $n = 3$); and EC_{50} was 1.4 ± 0.1 nM for activation of PLC-β3-Q by wild-type Gα$_q$ (800 ± 400-fold activation, $n = 2$). Maximum activation and absolute PLC activity vary among experiments because of variation in the preparation of substrate vesicles. *B*, the carbachol-stimulated lipase activity of PLC-β3-Q was assayed in reconstituted PE/PS/[^{3}H]PIP_2/cholesterol (16:10:1:2) vesicles that contained m1AChR, Gα$_q$-F, and Gβγ. An EC_{50} of 3.7 ± 0.3 nM ($n = 2$) was obtained, consistent with previous measurements for wild-type proteins (16). Data shown are from one of two experiments. *C*, the G_q GAP activity of PLC-β3-Q was assayed at steady state in PE/PS/cholesterol (9:5:1) vesicles reconstituted with 1.2 nM m1AChR, 1.4 nM wild-type Gα$_q$ and Gβγ. The EC_{50} was 4.1 ± 0.9 nM, again similar to that measured previously with wild-type proteins (3, 10, 16). Data shown here are the average and range (*error bars*) of duplicates from a single experiment.

(Fig. 2*A*), which is similar to the EC_{50} displayed by the unlabeled wild-type proteins (7, 11). A similar EC_{50} is observed for the G_q GAP activity of PLC-β3-Q (Fig. 2*C*). Such differences between EC_{50} and K_d, approaching 100-fold, were observed under identical experimental conditions, although the simplest models of allosteric regulation would predict that EC_{50} and K_d would be identical. We therefore set out to test the validity of the K_d measurement.

The discrepancy between EC_{50} and K_d is not caused by the mutation or covalent labeling of Gα$_q$-F and PLC-β3-Q, as shown by the activity data in Fig. 2 and the competition data in Fig. 1*D*. Maximal stimulation of the PLC activity of PLC-β3-Q by Gα$_q$-F–GTPγS is several hundred-fold (Fig. 2*A*), as is true for the two wild-type proteins under similar conditions (7). The fraction of Gα$_q$-F that bound GTPγS ranged among preparations between 50% and nearly 100%, as reported for wild-type Gα$_q$ (17). Further, in unilamellar phospholipid vesicles reconstituted with m1 muscarinic acetylcholine receptor (m1AChR), Gα$_q$-F, and Gβγ, the receptor catalyzed Gα$_q$-F activation by GTPγS with a rate constant of 0.5 s^{-1},[3] similar to that described previously for wild-type Gα$_q$ (16). The receptor-G_q-F vesicles also activated PLC-β3-Q in response to carbachol plus GTP, as described previously for the wild-type proteins (compare Fig. 2*B* with data of Biddlecome *et al.* (16)). Last, the G_q GAP activity of PLC-β3-Q was similar to that of wild-type PLC-β3, with the same EC_{50} (compare Fig. 2*C* with Biddlecome *et al.* (16) and Waldo *et al.* (10)).

To test whether the ~200 nM K_d obtained for PLC-β3-Q and Gα$_q$-F is sensitive to the specific placement of the donor and acceptor fluorophores, we prepared and studied the binding of two additional pairs of Gα$_q$–PLC-β3 FRET sensors. In one pair, the Gα$_q$-F donor was combined with PLC-β3 labeled with Alexa Fluor 594 maleimide at residue 720 (PLC-β3–720–Alx594). In the second, cerulean fluorescent protein was inserted as a FRET donor between residues Phe^{124} and Glu^{125} in Gα$_q$ (Gα$_q$-Cer), and the acceptor Alexa Fluor 594 maleimide was attached to Cys^{277} in the EF-hand domain of PLC-β3 (PLC-β3–277–Alx594). These two FRET pairs yielded similar values for K_d, specifically 210 ± 40 and 270 ± 60 nM (Fig. 3). Under identical assay conditions, the three FRET pairs yielded an average K_d of 250 ± 40 nM. In preliminary experiments, we constructed several other FRET pairs, listed in supplemental Table S1, and tested them at concentrations of acceptor-labeled PLC-β3 up to 50 nM. None yielded FRET signals consistent with a K_d below 50 nM.

In addition to the experiments described above, we also prepared Gα$_q$ labeled at residue 249 with the FRET acceptor Alexa

[3] N. Peddada and E. M. Ross, unpublished data.

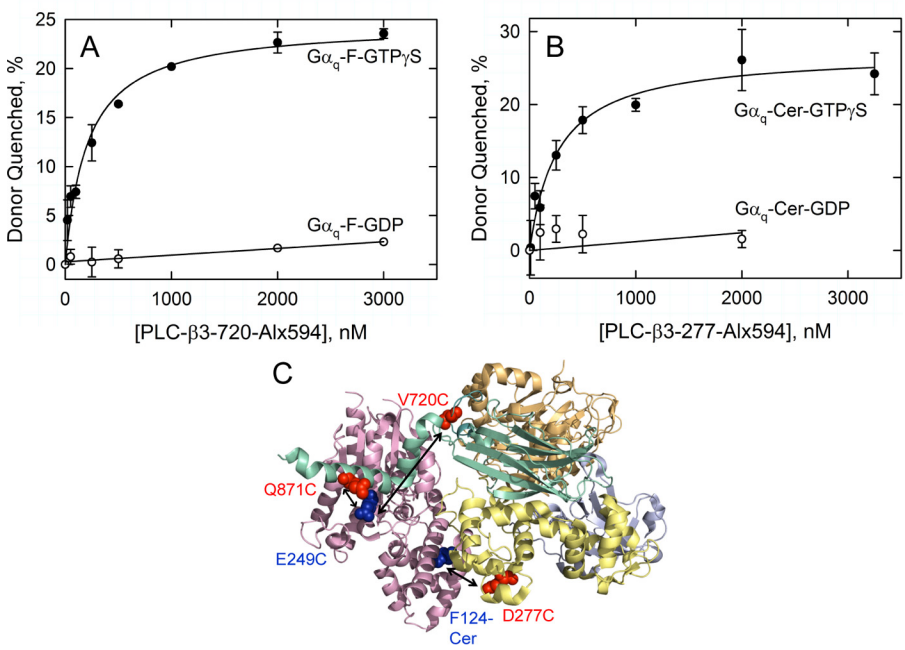

Figure 3. The affinity of GTPγS-activated Gα$_q$ for PLC-β3 does not depend on labeling position or label. *A*, binding of PLC-β3–720–Alx594 to 5 nM GTPγS-activated Gα$_q$-F (*closed circles*) was measured in a the presence of PE/PS vesicles with no added Ca^{2+}. Data are the average and range (*error bars*) from two independent experiments. The data were fit to a model of single-site binding to yield K_d = 210 ± 40 nM and donor quenching of 24.6 ± 1.1% at saturating PLC-β3–720–Alx594. In these experiments, Gα$_q$-F was 92% activated. Gα$_q$-F bound to GDP was not significantly quenched (*open circles*). *B*, binding of PLC-β3–277–Alx594 to 10 nM GTPγS-activated Gα$_q$-Cer (*closed circles*) was measured as in *A*, with K_d = 270 ± 60 nM and donor quenching of 27 ± 2% at saturation. Gα$_q$-Cer was 72% activated. Gα$_q$-Cer bound to GDP was not significantly quenched (*open circles*). *C*, crystal structure of the Gα$_q$–PLC-β3 complex (Protein Data Bank entry 3OHM) showing the location of fluorophores. Gα$_q$ is shown in *light pink*. The domains of PLC-β3 are *colored* as follows: PH domain (*gray*), EF hands (*yellow*), TIM barrel (*brown*), and C2 (*green*). The C-terminal helical domain is not shown. The sites on Gα$_q$ where FRET donors are attached are shown as *blue spheres*. Sites of FRET acceptor attachment on PLC-β3 are shown as *red spheres*. The *arrows* show the sites where donor and acceptor labels were attached in the three pairs of FRET sensors used to measure binding. In a broader screen of multiple fluorophore pairs (supplemental Table 1), no other pair that displayed FRET showed evidence of saturation <50 nM.

Fluor 594 and PLC-β3 labeled at residue 871 with the donor Alexa Fluor 488. This pair is identical to the Gα$_q$-F and PLC-β3-Q pair, but with donor and acceptor reversed. Although we were not able to add a high enough concentration of the Gα$_q$ acceptor to approach saturation, quenching of the PLC-β3 donor was consistent with $K_d \geq 200$ nM. Last, in an attempt to approximate the experiment of Runnels and Scarlata (25), we measured FRET from Gα$_q$-F to wild-type PLC-β3 that was uniformly labeled (14 cysteine residues) with Alexa Fluor 594 maleimide. For this pair, K_d in the presence of PC/PE/PS (1:1:1) vesicles was 560 ± 110 nM (n = 2; supplemental Fig. S1*D*). This high K_d presumably reflects partial inactivation of the PLC by alkylation, as we observed in enzymatic assays. Based on all of these data, the equilibrium affinity of Gα$_q$ binding to PLC-β3 does not reflect the location or chemical nature of the label, and affinity is confirmed by competition with unlabeled wild-type PLC-β3.

Equilibrium Gα$_q$–PLC-β3 binding measured by FCS

We next measured PLC-β3 binding to Gα$_q$ using FCS (26). Unlike FRET, FCS does not depend on the relative positions of the two fluorophores in the complex. In FCS, the fluorescence intensity in a small confocal volume is recorded as a function of time. Because the number of fluorescent particles in that volume is small, translational diffusion of fluorescent molecules in and out of the observation volume causes fluorescence intensity to fluctuate significantly relative to the time-averaged fluorescence. These fluctuations are autocorrelated using Equation 1 (see "Experimental procedures") (27), and the autocorrelation function, $G(\tau)$, decays to 1 as τ approaches infinity. The rate and shape of this decay depend on the diffusion coefficients of fluorescent species in the observation volume. When wild-type PLC-β3 (142 kDa) binds to Gα$_q$-F (42 kDa), the translational diffusion coefficient D of the labeled Gα$_q$ decreases significantly due to both the 4-fold increase in size of the Gα$_q$–PLC-β3 complex relative to Gα$_q$ and the asymmetry of the resulting complex (12).

As shown in Fig. 4*A*, $G(\tau)$ for GTPγS-activated Gα$_q$-F increased markedly in the presence of saturating PLC-β3. Fitting the values of $G(\tau)$ to Equation 2 showed that the diffusion coefficient D for Gα$_q$ decreased from 44 ± 4 $\mu m^2\ s^{-1}$ in the absence of PLC-β3 to 24.8 ± 1.7 $\mu m^2\ s^{-1}$ at saturating PLC-β3, a decrease of 44%. In these experiments, Gα$_q$-F was only 50% activated. Hence, the Gα$_q$-F diffusion coefficient of 24.8 ± 1.7 $\mu m^2\ s^{-1}$ obtained at saturating PLC-β3 concentrations was the average diffusion coefficient obtained for a mixture of free and PLC-β3–bound Gα$_q$-F. Diffusion coefficients of spherical particles with equal density are inversely proportional to the cube roots of their molecular masses. If Gα$_q$ and its complex with PLC-β3 were spherical, the diffusion coefficient of 42-kDa Gα$_q$ would be predicted to decrease by 37% upon binding 142-kDa PLC-β3. The slightly larger decrease in D presumably reflects the high asymmetry of the Gα$_q$–PLC-β3 complex (12).

Values of D for GTPγS-activated Gα$_q$ were then measured in the presence of increasing concentrations of PLC-β3 to deter-

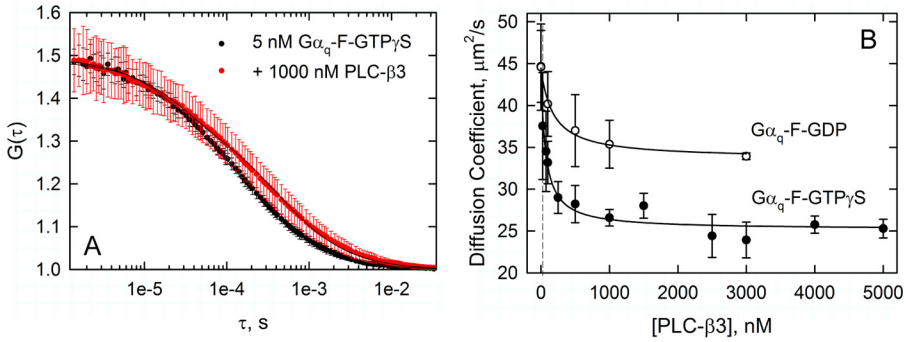

Figure 4. Gα_q–PLC-β3 binding measured by FCS. *A*, fluorescence autocorrelation curves obtained for GTPγS-activated Gα_q-F with 1000 nM (*red*) or without (*black*) PLC-β3. The data shown are from a single experiment and are the average and S.D. (*error bars*) of 50–60 autocorrelation curves, each obtained over 5 s. The data were fit to an equation with a single triplet state term and a single diffusion term (Equation 2). As GTPγS-activated Gα_q-F binds PLC-β3, the autocorrelation curves shift right due to a decrease in the diffusion coefficient of Gα_q-F. *B*, the diffusion coefficient of Gα_q-F bound to either GTPγS (*closed circle*) or GDP (*open circle*) at increasing concentrations of PLC-β3. The data shown are the average and S.D. of three independent experiments. A K_d of 120 ± 20 and 240 ± 60 nM was obtained for PLC-β3 binding to Gα_q–GTPγS and Gα_q–GDP, respectively.

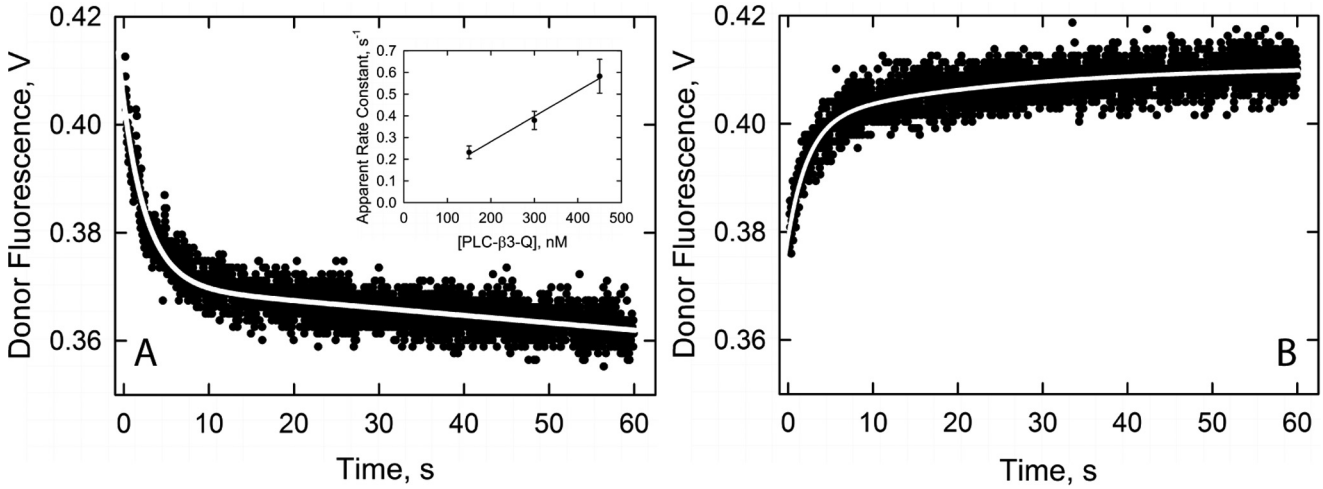

Figure 5. Rates of Gα_q–GTPγS–PLC-β3 association and dissociation. Association and dissociation rates of GTPγS-activated Gα_q-F and PLC-β3-Q in the presence of PE/PS vesicles were measured at 25 °C by stopped-flow FRET. *A*, to measure association, quenching of donor fluorescence was followed upon the addition of PLC-β3-Q (300 nM) to GTPγS-activated Gα_q-F (5 nM). Data were fit to a rate equation with a single exponent plus a linear term that accounts for photobleaching, which is also seen with Gα_q-F alone. *Inset*, pseudo-first-order association rate constants obtained at 150, 300, and 450 nM PLC-β3-Q were fit to yield a second-order association rate constant of 1.2×10^6 M^{-1} s^{-1} and an extrapolated dissociation rate constant of 0.05 ± 0.03 s^{-1}. Each data point shown in the *inset* is the average and S.D. (*error bars*) of association rates derived from four independent experiments, each with 12 mixing curves of the sort shown in *A* at each PLC concentration. Rates did not vary with substoichiometric concentrations of Gα_q-F. Gα_q-F used in these experiments was 40–50% activated. *B*, to measure dissociation, recovery of donor fluorescence was measured upon the addition of 1.8 μM unlabeled wild-type PLC-β3 to a mixture of 5 nM GTPγS-activated Gα_q-F (25 nM in some other experiments) and 250 nM PLC-β3-Q. The data shown are representative of 13 fluorescence recovery curves obtained from three independent experiments. The data were fit to a bi-exponential rate equation with a fast dissociation rate constant of 0.60 ± 0.17 s^{-1} that accounts for 67 ± 5% of the fluorescence recovery and a slower rate of 0.05 ± 0.02 s^{-1} that accounts for 33 ± 5% of the recovery.

mine their binding affinity (Fig. 4*B*). The decrease in D of Gα_q-F upon PLC-β3 binding was well fit by a simple bimolecular binding function to yield K_d = 120 ± 20 nM. This value corresponds well to the value of K_d that was determined by FRET in the same aqueous buffer or in buffer with 0.2% cholate. The observed affinity of PLC-β3 binding to Gα_q is thus the same when measured by either intermolecular FRET or by FCS.

The diffusion coefficient of GDP-bound Gα_q-F also decreased at high PLC-β3 concentrations, but only by 23%, with an apparent K_d of 240 ± 60 nM (Fig. 4*B*). This is about half the decrease observed with the 50% activated Gα_q-F. These data might suggest a second, lower-affinity binding mode to create a complex with a different hydrodynamic radius. If this hypothetical binding site were near the PLC-β3 C terminus, our FRET sensors would have been too far apart to detect the interaction.

Association and dissociation kinetics of Gα_q and PLC-β3

To determine the kinetic behavior of Gα_q–PLC-β3 binding, we used stopped-flow FRET to measure the association and dissociation rates for Gα_q-F and PLC-β3-Q. To measure association, donor quenching was followed upon the addition of PLC-β3-Q (150, 300, or 450 nM) to GTPγS-activated Gα_q-F (5 or 25 nM) at 25 °C in the presence of 250 μM PE/PS (4:1) vesicles and no added Ca^{2+} (Fig. 5*A*). Data were fit to a single exponential and a linear term to account for minor photobleaching. The pseudo-first order association rate increased with increasing PLC-β3-Q concentration, yielding a second-order association rate constant, k_{on}, of $1.2 \pm 0.2 \times 10^6$ M^{-1} s^{-1} (Fig. 5*A*, *inset*). These data also yielded an extrapolated dissociation rate constant k_{off} of 0.05 ± 0.03 s^{-1}. Dissociation was measured independently under identical conditions by monitoring recovery of

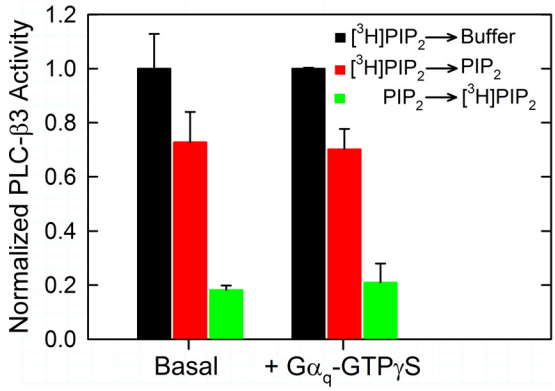

Figure 6. PLC-β3 and Gα$_q$ "hop" freely among vesicles. The sequential addition of substrate vesicles containing either [^{3}H]PIP$_2$ or non-tritiated PIP$_2$ was used to determine whether Gα$_q$–GTPγS and PLC-β3 can move freely among vesicles over the time course of PLC assays. Gα$_q$–GTPγS (5 nM) or buffer (basal) was incubated with either [^{3}H]PIP$_2$ vesicles (*black*, *red*) or unlabeled PIP$_2$ vesicles (*green*) for 30 min on ice. The reaction was started by adding PLC-β3 and warming to 37 °C. Ten minutes into the reaction, additional reaction buffer (*black*), unlabeled PIP$_2$ vesicles (*red*), or [^{3}H]PIP$_2$ vesicles (*green*) were added. Reactions were terminated at 30 min, and [^{3}H]IP$_3$ was measured as described. After the second addition at 10 min, the total lipid concentration in all samples was 262 μM. In samples with a mixture of [^{3}H]PIP$_2$ vesicles and unlabeled PIP$_2$ vesicles (*red* and *green*), the concentration of [^{3}H]PIP$_2$ vesicles was equal to that of unlabeled PIP$_2$ vesicles. PLC activities were calculated as mol of [^{3}H]IP$_3$ produced/min/mol of PLC and were normalized to the activities obtained with just [^{3}H]PIP$_2$ vesicles (*black*). For both basal and Gα$_q$-stimulated samples, initial incubation with unlabeled vesicles and a subsequent 20-min incubation with [^{3}H]PIP$_2$ vesicles (*red*) produced 70% as much [^{3}H]IP$_3$ as did incubation for the full 30 min with only [^{3}H]PIP$_2$ vesicles (*black*), similar to the 67% predicted if both PLC-β3 and Gα$_q$ move freely among vesicles. For the opposite order of addition (*green*), basal and stimulated activities were 20% of control, approximately consistent with the expected 33%. Data are the average and range (*error bars*) of duplicates from a single experiment in which basal activity was 1.1 ± 0.1 min^{-1} and Gα$_q$-stimulated activity was 555 ± 1.3 min^{-1} and are representative of three similar experiments.

donor fluorescence upon the addition of excess, unlabeled PLC-β3 (1.8 μM) to a mixture of Gα$_q$-F (5 or 25 nM) and PLC-β3-Q (250 nM). These fluorescence recovery data were not fit well by a single exponent (see "Experimental procedures"). A two-exponent fit yielded a principal dissociation rate constant, k_{off}, of 0.60 ± 0.17 s^{-1} that accounted for 67 ± 5% of the recovery and a slower dissociation rate of 0.05 ± 0.02 s^{-1}, probable drift, that accounted for the remainder. The slower value agrees with the extrapolated k_{off} obtained from the association data in Fig. 5*A*. These two rates bracket the dissociation rate of 0.3 s^{-1} measured in cells by Jensen *et al.* (28). A k_{on} of 1.2 × 10^6 M^{-1} s^{-1} and the major k_{off} of 0.6 s^{-1} yield a kinetically determined K_d = 500 nM, but even the slower value of k_{off} yields a K_d that is still more than 10-fold higher than the EC_{50}. Hence, the kinetic parameters yield a K_d similar to that obtained directly from equilibrium binding measurements using either FRET or FCS.

Gα$_q$ and PLC-β3 binding to phospholipid vesicles

The interaction of PLC-β and Gα$_q$ could be strongly influenced by their simultaneous binding to phospholipid vesicles, where relevant PLC activation occurs. We used classical order-of-addition experiments to show that the binding of these two proteins to phospholipid substrate vesicles is reversible, in that they display some component of "hopping" kinetics (29) in addition to their "scooting" on the surface of individual vesicles over the time frame of both activity and binding assays (Fig. 6).

We also used FCS to confirm that Gα$_q$ and PLC-β3 each bind to phospholipid vesicles and that their binding is rapidly reversible (Fig. 7). Fluorescence autocorrelations were measured for 7.5 nM PLC-β3–Alx488 (labeled at position 871) (Fig. 7*A*) and 5 nM Gα$_q$-F (Fig. 7*B*) in the absence or presence of 250 μM PE/PS (4:1) vesicles. Autocorrelation curves obtained for each protein were markedly right-shifted in the presence of vesicles (Fig. 7), indicating a significant decrease in the diffusion coefficient of each protein due to vesicle binding. To determine the fraction of protein bound to vesicles, autocorrelation data (Fig. 7, *red circles*) were fit to an equation with two sets of diffusion and triplet state terms (Equation 3), one each for the population of free protein and protein bound to vesicles (Equation 4). This analysis indicated that 56 ± 6 and 44.5 ± 0.4% of PLC-β3–Alx488 and Gα$_q$–Alx488, respectively, were bound to vesicles. These values indicate that both proteins can freely exchange between vesicles and the aqueous medium, consistent with the hopping kinetics observed for PLC stimulation.

Relationship of K_d and EC_{50}

Several recognized molecular mechanisms of enzyme activation can give rise to an EC_{50} that is significantly smaller than the equilibrium K_d for activator-enzyme binding, and we have considered three for possible involvement in the Gα$_q$–PLC-β3 system.

Classically, "essential allosteric activation," in which activator is required for enzyme–substrate binding (24), can produce $EC_{50} \ll K_d$ but requires that substrate concentration be well above K_m for this behavior. Because the concentrations of PIP$_2$ used here are well below K_m (Biddlecome *et al.* (16); confirmed here), this mechanism does not apply. A second set of mechanisms that can produce $EC_{50} \ll K_d$ involves enzyme oligomerization with strongly negatively cooperative ligand binding. However, a disagreement of 50–100-fold, the sort observed here, would require very high stoichiometries of oligomerization to completely obscure the initial, highest-affinity binding event. No evidence of such oligomerization has been obtained, and Waldo *et al.* (10) found that PLC-β3 behaves as a monomer according to size-exclusion chromatography. Whereas we found variable formation of an apparent dimer of PLC-β1 in pilot analytical ultracentrifugation experiments, we also found that most protein behaved as a monomer. Singer *et al.* (8) demonstrated formation of a dimer of the C-terminal helical domain of turkey PLC-β2 during crystallization, and the importance of the dimer interface was supported by the effect of mutagenesis (20). Based on this work, we introduced novel cysteine residues (S1042C, H1104C, and Q1157C) in the PLC-β3 C terminus to probe oligomerization by FRET. No changes in donor fluorescence were observed when PLC-β3 S1042C–Alx549 (0–500 nM) was added to PLC-β3 H1104C–Alx488 (2.5 nM) or when PLC-β3 Q1157C–Alx594 (0–750 nM) was added to PLC-β3 Q1157C–Alx488 (1 nM), with or without 100 nM Gα$_q$–GTPγS. Each pair is separated by 15 Å in the turkey PLC-β C terminus crystal structure (8), well within the Förster distance for these fluorophores. In summary, we find no evidence for higher-order oligomerization as an origin of the high K_d observed for Gα$_q$ binding to PLC-β3.

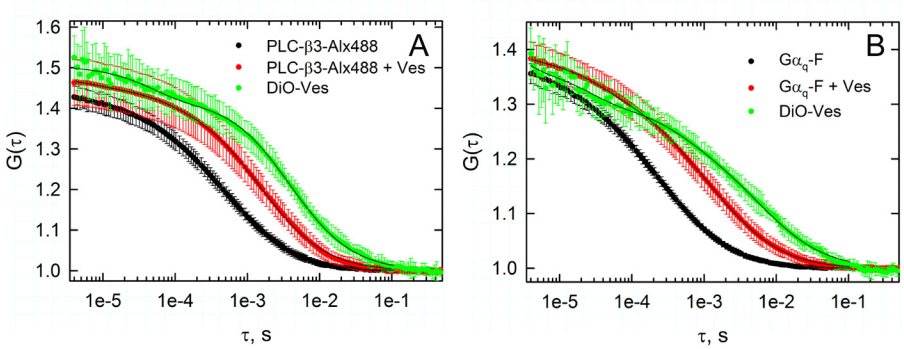

Figure 7. PLC-β3 and Gα$_q$ bind phospholipid vesicles. FCS data, expressed as $G(\tau)$, were obtained for 7.5 nM PLC-β3–Alx488 (*A*) and 5 nM Gα$_q$-F (*B*), both alone (*black*) and in the presence of 250 μM PE/PS (4:1) vesicles (*red*). FCS data were also obtained for vesicles labeled with DiO (*green*). $G(\tau)$ values shown are the average and S.D. (*error bars*) for ~10 (vesicles) and 40–50 (proteins alone and with vesicles) autocorrelation curves (5-s acquisition). $G(\tau)$ values obtained for protein alone (*black*) and for DiO-labeled vesicles (*green*) were fit to an equation with one diffusion term and one triplet state term (Equation 2). The diffusion coefficient for free PLC-β3–Alx488 was 24 ± 3 μm^2 s^{-1} ($n = 4$), and the diffusion coefficient for free Gα$_q$-F was 44 ± 4 μm^2 s^{-1} ($n = 8$). $G(\tau)$ obtained for mixtures of fluorescent proteins and vesicles (*red*) were fit to an equation (Equation 3) with two sets of diffusion and triplet state terms, each corresponding to the population of free protein and protein bound to vesicles. Diffusion and triplet state parameters for free proteins were fixed at values obtained with protein alone. Amplitudes obtained for the population of free protein in the mixture were used to calculate the fraction of protein bound to vesicles. The diffusion coefficient of vesicle-bound PLC-β3–Alx488 was found to be 6.2 ± 1.1 μm^2 s^{-1}, with 56 ± 6% of the protein bound to vesicles. The diffusion coefficient of vesicle-bound Gα$_q$-F bound to vesicles was 6.5 ± 0.3 μm^2 s^{-1}, with 44.5 ± 0.4% bound to vesicles. The diffusion coefficients for the two vesicle-bound proteins were essentially identical and similar to the diffusion coefficient determined for DiO-labeled vesicles alone (4.3 ± 1.1 μm^2 s^{-1}). The slightly higher value of D for vesicle-bound protein may reflect protein binding to smaller vesicles. The *green* $G(\tau)$ *curves* are not unimodal, indicating size heterogeneity.

Hysteretic PLC activation is a more likely mechanism. If PLC-β3 remains active for some time after it dissociates from Gα$_q$–GTPγS (or after Gα$_q$ is deactivated but perhaps remains bound), EC_{50} will be lower than K_d. In such a mechanism, the PLC-β3 deactivation rate, k_{deact}, is slower than the Gα$_q$–GTPγS dissociation rate (k_{off}). Thus, EC_{50}, the ratio of the deactivation and activation rate constants k_{deact}/k_{act}, is lower than K_d, the ratio of dissociation and association rate constants k_{off}/k_{on}. Because k_{act} cannot be faster than k_{on}, EC_{50} is less than K_d. Such a hysteretic PLC-β3 activation/deactivation cycle allows Gα$_q$ to behave formally as a catalyst of PLC activation. To determine whether PLC-β3 displays such hysteresis, we compared the rate of dissociation of Gα$_q$–GTPγS from PLC-β3 (k_{off}, measured as described above) with the rate of PLC-β3 deactivation following its dissociation from Gα$_q$–GTPγS (k_{deact}). Dissociation of Gα$_q$–GTPγS and consequent dissociation of the active complex was initiated by the addition of an excess of a catalytically inactive PLC-β3 mutant to sequester free Gα$_q$–GTPγS as it dissociates. PLC-β3 H332A,H379A, which lacks the two catalytic histidine residues, does not hydrolyze PIP_2 but competitively inhibits activation of wild-type PLC-β3 by Gα$_q$–GTPγS with a K_i that is equal to the EC_{50} for activation of the wild-type enzyme (Fig. 8*A*). Gα$_q$–GTPγS–stimulated PLC-β3 activity was measured before and after the addition of excess H332A,H379A PLC-β3 (Fig. 8*B*), and the rate of PLC deactivation was used to determine the deactivation lifetime ($\tau_{deact} = 1/k_{deact}$), as described by Cassel *et al.* (30). The calculated value of τ_{deact} was 0.3 ± 4.7 s ($n = 3$), which was too short to be measured accurately but which places a lower bound on k_{deact} of ~3 s^{-1}. This value is actually faster than the dissociation rate constant of 0.6 s^{-1} obtained for Gα$_q$–GTPγS and PLC-β3 (Fig. 5*B*), indicating that PLC-β3 hysteresis of this sort is not responsible for the discrepancy between EC_{50} and K_d.

In cells, however, it is likely that hydrolysis of Gα$_q$-bound GTP is the initial deactivating event in signal termination rather than the dissociation of GTP-activated Gα$_q$ from PLC-β. Thus, slow deactivation of PLC bound to Gα$_q$–GDP might provide an alternative hysteretic mechanism to account for $K_d > EC_{50}$. We therefore compared the rate of Gα$_q$ deactivation promoted by the GAP activity of PLC-β with the rate of consequent deactivation of PLC-β3-catalyzed PIP_2 hydrolysis to see whether PLC deactivation is delayed, another possible source of hysteresis. We previously showed that the PLC-β–promoted hydrolysis of Gα$_q$–GTP occurs with a rate of ~10 s^{-1} in a system of unilamellar phospholipid vesicles reconstituted with m1AChR and G_q (3). Here, we measured the rate of PLC-β3 deactivation following Gα$_q$ deactivation in the same reconstituted system. PLC-β3 activity was first allowed to reach receptor-stimulated steady-state in the presence of GTP and the agonist carbachol. To initiate deactivation, the antagonist atropine and excess GDP were added, and PLC-β3 activity was measured for several minutes thereafter. Deactivation lifetimes were calculated as in Fig. 8*B* (30). As shown in Fig. 9, deactivation lifetimes are relatively long when the concentration of Gα$_q$ is greater than that of PLC-β3 because excess Gα$_q$–GTP must be sequentially turned off by a limiting amount of PLC-β3. At PLC-β3 concentrations that were equal to or greater than the steady-state concentration of GTP-activated Gα$_q$, the time constant for PLC-β3 deactivation approached 2.7 ± 1.6 s, which corresponds to a lower bound for the rate, $k_{deact} \geq 0.4$ s^{-1}. This rate is about 25-fold slower than the previously measured rate of GTP hydrolysis. This difference alone is not slow enough to account for the nearly 100-fold difference between EC_{50} and K_d for the interaction of Gα$_q$ and PLC-β3 but could partially explain the discrepancy between the EC_{50} and K_d.

Discussion

We set out to measure the thermodynamics and kinetics of PLC-β3 binding to Gα$_q$ to define the biochemical mechanisms of their mutual regulation. Activation of PLC-β by Gα$_q$ is widely thought to be a classical allosteric event, as is the G_q GAP activity of PLC-β (7). If classical allostery were the mechanism

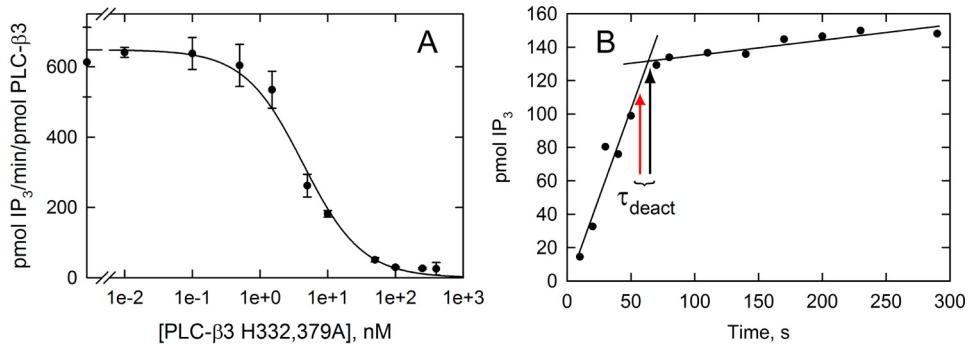

Figure 8. PLC-β3 deactivation following PLC-β3 dissociation from $G\alpha_q$–GTPγS. *A*, the catalytically inactive H332A,H379A PLC-β3 inhibits $G\alpha_q$–GTPγS–stimulated PLC-β3 activity. The data are the average and range (*error bars*) of duplicates from a single experiment with a fit to a single-site competitive inhibition equation. An IC_{50} of 3.2 ± 1.6 nM was obtained from two independent experiments using 5 nM $G\alpha_q$–GTPγS and 1 nM PLC-β3. Given an EC_{50} of 3 nM, $IC_{50} \approx K_i$. *B*, the PLC-β3 deactivation lifetime, τ_{deact}, was measured at 25 °C by following the activity of 1 nM PLC-β3 stimulated by 5 nM $G\alpha_q$–GTPγS before and after quenching of activation by 600 nM H332A,H379A PLC-β3 (*red arrow*). The deactivation time is given by the difference between the time at which H332A,H379A PLC-β3 was added and the time at which the linear extrapolations of the initial and final rates intersect (*black arrow*) (30). These deactivation times were too fast to measure accurately. In three independent experiments, approximate values were 4 s (shown), 2 s, and −5 s.

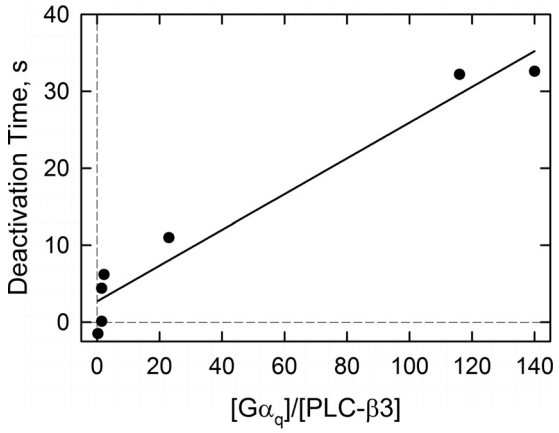

Figure 9. PLC-β3 deactivation following GAP-catalyzed deactivation of GTP-activated $G\alpha_q$. The deactivation lifetime of PLC-β3 following $G\alpha_q$ deactivation was measured at 30 °C in a reconstituted vesicle system consisting of m1AChR, $G\alpha_q$, and G$\beta\gamma$. Vesicles were allowed to reach steady state in the presence of carbachol and GTP. Activation was terminated at zero time by the addition of the m1AChR antagonist, atropine, and excess GDP. PLC-β3 activity was measured before and after termination, and the PLC-β3 deactivation lifetime was obtained using the method described by Cassel *et al.* (30), similar to that shown in Fig. 8*B*. Deactivation lifetimes were measured at different concentration ratios of $G\alpha_q$ and PLC-β3. At higher $G\alpha_q$/PLC-β3 ratios, τ_{deact} is longer, indicating that the rate-limiting step in PLC-β3 deactivation is the sequential deactivation of excess $G\alpha_q$–GTP molecules by the GAP activity of substoichiometric PLC-β3. We obtained an estimate of PLC-β3's intrinsic deactivation lifetime by plotting τ_{deact} as a function of the $G\alpha_q$/PLC-β3 ratio and extrapolating to $G\alpha_q$/PLC-β3 = 0, to yield τ_{deact} = 2.7 ± 1.6 s. This value is an upper bound. The data points are observed deactivation times for individual experiments. Three different vesicle preparations were used to obtain the data shown. In these experiments, m1AChR concentrations varied from 0.62 to 2.7 nM, as determined by [^{3}H]quinuclidinylbenzilate binding. $G\alpha_q$ concentrations varied from 0.5 to 3.5 nM as determine by carbachol-stimulated [^{35}S]GTPγS binding (16).

of this bidirectional regulation, then the K_d for $G\alpha_q$ binding to PLC-β should be equal to the EC_{50} values for the two activities. Both EC_{50} values, for PLC-β activation by $G\alpha_q$ and acceleration of G_q-GTP hydrolysis by PLC-β activation, are 2–5 nM (7, 10, 11, 16, 17). Hence, the corresponding K_d was expected to be in the same, low nanomolar range. Surprisingly, the data presented here show that the K_d for PLC-β3 binding to $G\alpha_q$–GTPγS is in the range of 130–250 nM, almost 2 orders of magnitude higher (Table 1).

The unexpectedly high value of K_d determined here appears to be correct according to multiple criteria. First, binding affinity was determined by two distinctly different techniques: measurement of FRET between single fluorophores covalently bound to PLC-β3 and $G\alpha_q$ and FCS measurement of retardation of diffusion of fluorescently labeled $G\alpha_q$ by unlabeled PLC-β3. Because the FRET measurement is simpler, we were also able to perform several other controls in that format. Binding was competitively inhibited by unlabeled PLC-β3 with K_i equal to the K_d determined directly by FRET, and the G_q-unresponsive L859E mutant PLC-β3 did not inhibit. Only the GTPγS-activated form of $G\alpha_q$ bound PLC-β3 with significant affinity. Binding affinity was not changed by the choice of fluorophore bound to PLC-β3 or by substitution on $G\alpha_q$ of cerulean fluorescent protein in place of a covalently bound synthetic fluorophore. Labeling of PLC-β3 or $G\alpha_q$ at multiple positions on each molecule that are close by in the complex reported the same affinity. Last, binding affinity was not greatly altered by precise experimental conditions: the presence or absence of phospholipid vesicles with or without the PLC substrate PIP_2, the inclusion of detergent, or the presence of Ca^{2+}, which is required for the PLC reaction. Last, the ratio of the dissociation rate constant to the association rate constant, measured by stopped-flow FRET, was approximately equal to the equilibrium dissociation constant (*i.e.* $K_d = k_d/k_a$. Our data thus indicate that the K_d for PLC-β3 binding to $G\alpha_q$ is about 200 nM and clearly much higher than EC_{50} values determined here or previously.

The K_d value of ~200 nM reported here agrees with K_d values of 206 and 108 nM (two experiments) that were determined by Waldo *et al.* (10), who used surface plasmon resonance to measure the affinity of PLC-β3 for an Al^{3+}/F^--activated $G\alpha_i$–$G\alpha_q$ chimera, which activates PLC-β.

In contrast, Runnels and Scarlata (25) obtained much lower K_d values for $G\alpha_q$ binding to three different PLC-β isoforms. They used intermolecular FRET between wild-type $G\alpha_q$ labeled with an amine-reactive coumarin and wild-type PLC-β covalently labeled with a thiol-reactive quencher (dabcyl). In that study, binding measured in the presence of PC/PE/PS (1:1:1) vesicles yielded K_d values of <10 nM for $G\alpha_q$–GTPγS and PLC-β1, -β2, or -β3, which are similar to values of EC_{50} for PLC activation that have been measured by us and others. However, when we measured binding of $G\alpha_q$-F–Alx488 to wild-type

PLC-β3 labeled with a thiol-reactive Alexa Fluor 594 in the presence of PC/PE/PS vesicles, we found K_d = 560 ± 110 nM (supplemental Fig. S1*D*), about 2–3-fold higher than in our other measurements. We did not try to emulate the Gα$_q$ donor used by Runnels and Scarlata (25) because we found that non-selective amine labeling inactivates Gα$_q$[4] and because subsequent dialysis against 0.1 M $(NH_4)_2SO_4$, which they used to remove unreacted fluorophore, would irreversibly inactivate Gα$_q$ (31).

Studies of other proteins that activate PLC-β have also yielded physically determined values of K_d much above the published EC_{50}. Such disagreement may therefore be general and mechanistically informative for the PLC-β family. Gβγ activates PLC-β3 with an EC_{50} of ~30 nM (7, 19). However, FRET measurements of PLC-β3 binding to Gβγ in the presence of phospholipid vesicles yielded a K_d of 220 ± 46 nM (19), ~7-fold higher than the EC_{50}. Similarly, Rac1 activates PLC-β2 with EC_{50} ~6 nM (19), but surface plasmon resonance measurements of GTPγS-bound Rac2 binding to PLC-β2 yielded K_d ~5 μM (32), ~1000-fold higher than the EC_{50}. Although this latter comparison spans two laboratories, and the binding measurement used non-prenylated Rac1, the 1000-fold discrepancy is still striking. Hence, there may be a common and general mechanism by which potent activation of PLC-β isoforms is achieved despite much weaker equilibrium binding affinity of PLC-β for its activators.

Phospholipid bilayers, with or without PIP_2 or Ca^{2+}, had little effect on the affinity of PLC-β3–Gα$_q$ binding as measured by intermolecular FRET (Figs. 1*B* and 3 (*A* and *B*), supplemental Fig. S1 (*A–C*), and Table 1). The addition of 0.2% cholate also had little effect (supplemental Fig. S1*B*). FCS measurements of PLC-β3–Gα$_q$ binding in aqueous buffer yielded a K_d of 120 ± 20 nM (Fig. 4*B*), consistent with the FRET measurements in the different media. Thus, PLC-β3 binding to Gα$_q$ in aqueous buffer or detergent solution is at least as tight as that measured in the presence of phospholipid vesicles, which suggests that permanent vesicle binding does not confine both proteins to a restricted annular membrane surface volume. This conclusion is consistent with FCS measurements of Gα$_q$ and PLC-β3 diffusion in the absence and presence of phospholipid vesicles, which showed that just less than half of each protein is bound to vesicles at equilibrium (Fig. 7). It is also consistent with the substantial amount of protein exchange among vesicles during the PLC assay (Fig. 6).

Gα$_q$ is palmitoylated at residues Cys^9 and Cys^{10}, and knockdown of a Gα$_q$ palmitoyl acyl-transferase causes Gα$_q$ to relocalize from the plasma membrane to the cytoplasm and disrupts Gα$_q$ signaling (33). Cys^9 and Cys^{10} were retained in all Gα$_q$ variants used in this work, and only the fraction of Gα$_q$ that was both membrane-localized and attached to Gβγ was purified (see "Experimental procedures"). We do not know whether Gα$_q$ loses any palmitate during purification. Fluorescent maleimide labeling of Gα$_q$ variants yielded 2 dye molecules bound per protein, suggesting that one of the cysteine residues at position 9 or 10 remains palmitoylated.

[4] S. Nayak, P. Navaratnarajah, and E. M. Ross, unpublished data.

Of the multiple regulatory mechanisms that can produce an EC_{50} value below the K_d for the activator, the most likely in this case seemed to be slow deactivation of PLC-β after dissociation from Gα$_q$ or the other protein activators mentioned above. Because the rate of activation cannot be faster than the binding rate, slow deactivation would lead to a lower than expected EC_{50}. To test whether PLC-β3 activation displays such hysteresis, we compared the rate of dissociation of the Gα$_q$–PLC-β3 complex (Fig. 5*B*) with the rate of PLC-β3 deactivation after dissociation (Fig. 8*B*). No such hysteresis was detected. The PLC-β3 deactivation lifetime following dissociation varied between 2 and 5 s, and the dissociation lifetime itself was 1.5 ± 0.3 s. The PLC-β3 deactivation lifetime following GAP-catalyzed Gα$_q$ deactivation was also found to have an upper limit of ~3 s (Fig. 9), consistent with the dissociation lifetime of 3.6 s measured in cells (28). For a simple hysteretic mechanism to produce a K_d/EC_{50} ratio of about 100, the PLC-β3 deactivation rate would have to be 100-fold slower than the dissociation rate. The simplest version of this mechanism, therefore, does not explain our data.

A second mechanism that yields $K_d \gg EC_{50}$ is one in which the acceleration of an initially rate-limiting partial reaction in the catalytic pathway is accelerated to the point where a second partial reaction becomes limiting. Further stimulation by increased fractional binding of activator is therefore without effect, and activation saturates at ligand concentrations well below those needed to saturate binding. Classical examples are referred to as "essential" and "non-essential" activation, where the second partial reaction is substrate binding and the substrate concentration is well above K_m (24). In the case of PLC-β, however, the concentration of PIP_2 is substantially below K_m (16) (confirmed in this study). Therefore, this set of mechanisms is also not applicable.

We cannot definitively propose a mechanism to account for the surprisingly high ratio of K_d/EC_{50} that we observe for the Gα$_q$–PLC-β interaction, but we believe it to have a kinetic basis. We have noted that Gα$_q$-stimulated PLC activity displays a definite lag period before maximal activity is attained. This lag can be 5–30 s in duration, depending upon assay conditions, and we have had to choose assay duration and PLC concentration carefully to ensure steady state for PLC assays where activities varied over a large range (*cf.* Ref. 7). We do not know the physical origin of this lag, but it may be related to the low value of k_{off} that is obtained by extrapolating the pseudo-first-order association rate constant to zero PLC-β3 concentration (Fig. 5, compare *A* (*inset*) with the value obtained in *B* and related dissociation measurements). This lower value may reflect the second phase of dissociation noted in Fig. 5*B*. Together, they suggest the existence of a transient, active state of the PLC that is hysteretic in its decay after Gα$_q$ dissociation, but on a time scale shorter than the 2-s window that we are able to explore. This transient active state may relate to the two-step deactivation process proposed by Waldo *et al.* (10). This state may also be the one favored by Gβγ, which also activates PLC-β with an EC_{50} lower than the observed K_d (19) and which activates synergistically with Gα$_q$ (7).

Experimental procedures

Proteins

Human PLC-β3 with an N-terminal His_6 tag was purified from *Escherichia coli* as described previously (19). Solvent-exposed cysteine residues at positions 193, 516, 614, 892, 1005, and 1207 were mutated to serine by QuikChange mutagenesis (19). Additional point mutations were introduced in this background.

Cysteine residues were introduced in place of Asp^{277}, Val^{720}, or Gln^{871} in PLC-β3 for fluorescence labeling with thiol-reactive probes. Before labeling, PLC-β3 was buffer-exchanged into 20 mM NaHEPES (pH 7.5), 100 mM NaCl, 10% glycerol to remove DTT. The protein (50–100 μM) was then incubated with either Alexa Fluor 488 C_5 maleimide or Alexa Fluor 594 C_5 maleimide (250 μM) for 1 h on ice. The reaction was quenched using 1 mM β-mercaptoethanol, and protein was adsorbed to SP Sepharose in 20 mM NaMES buffer (pH 6.0), 10% glycerol, and 1 mM β-mercaptoethanol. The resin was washed with this buffer supplemented with 100 and 250 mM NaCl to remove free dye. Labeled PLC-β3 was eluted with 450 mM NaCl and exchanged into PLC-β3 storage buffer (20 mM NaHEPES (pH 7.5), 100 mM NaCl, 0.1 mM EDTA, 0.1 mM DTT, 10% glycerol), frozen in liquid N_2, and stored at −80 °C. To determine labeling ratios, dye concentrations were measured by absorbance (Alexa Fluor 488 C_5 maleimide: λ_{max} = 495 nm, ϵ = 73,000 cm^{-1} M^{-1}; Alexa Fluor 594 C_5 maleimide: λ_{max} = 590 nm, ϵ = 92,000 cm^{-1} M^{-1}), and protein concentrations were determined by Amido Black binding (34). Labeling ratios were consistently between 1 and 2 dye molecules/protein.

To create a catalytically inactive PLC-β3 mutant, histidine residues at positions 332 and 379 in PLC-β3 (35) were mutated to alanine by QuikChange mutagenesis. Purified PLC-β3-L859E (10), a PLC-β3 variant that cannot bind or be activated by $G\alpha_q$, was a kind gift from John Sondek (University of North Carolina).

Human $G\alpha_q$ cDNA in which three of the protein's five cysteine codons (at positions 144, 219, and 330) had been mutated to alanine was a gift from Jürgen Wess (National Institutes of Health) (36). Cysteines at positions 9 and 10, which are subject to palmitoylation and are necessary for maximal PLC-β activation (37), were retained. To create $G\alpha_q$ FRET sensors, a cysteine residue was introduced in place of Glu^{249} in $G\alpha_q$ ($G\alpha_q$-E249C) for fluorescence labeling. $G\alpha_q$ with cerulean fluorescent protein (38) inserted between residues Phe^{124} and Glu^{125} ($G\alpha_q$-Cer) was used as a FRET donor in some experiments.

$G\alpha_q$ constructs were expressed and purified essentially according to Biddlecome *et al.* (16, 39) but with some alterations. To express $G\alpha_q$ FRET constructs, Sf9 insect cells were infected with baculoviruses encoding Ric8A-GST, $G\beta_2$-His_6, $G\gamma_2$-His_6, and either $G\alpha_q$-E249C or $G\alpha_q$-Cer. A single baculovirus encoding both wild-type $G\alpha_q$ and $G\gamma_2$-His_8 was made using the pFastBac-Dual shuttle vector (Invitrogen). To express wild-type $G\alpha_q$, Sf9 cells were infected with baculoviruses encoding $G\alpha_q$–$G\gamma_2$-His_8, $G\beta_2$-His_6, and Ric8A-GST. Ric8A was co-expressed to improve $G\alpha_q$ expression (39), but the soluble form of $G\alpha_q$ that is bound to Ric8A activates PLC-β poorly (19, 39). According to immunoblots, almost all Ric8A was removed during membrane preparation, and the remainder was removed upon adsorption of the $G\alpha_q$–$G\gamma_2$-His_8–$G\beta_2$-His_6 trimer to NTA-Ni^{2+}–agarose (below). Cells were harvested at 4 °C ~50 h after infection. Only $G\alpha_q$ that was both membrane-localized and initially bound to Gβγ was purified. All purification steps were performed on ice or at 4 °C. Cells were resuspended in ice-cold lysis buffer (20 mM Tris (pH 8), 3 mM $MgCl_2$, 2 μg/ml leupeptin, 1 μg/ml aprotinin, 200 μM PMSF, and 24 μg/ml DNase) at 15 ml of lysis buffer/g of cells. Following Dounce homogenization, the cell lysate was centrifuged at 30,000 × *g* for 25 min. The resulting pellet was resuspended in 3.5 ml of lysis buffer/g of cells, homogenized, and again centrifuged at 30,000 × *g* for 25 min. The membrane pellet was finally resuspended in 2 ml of lysis buffer/g of cells. Protein concentration of the membrane lysate was measured by the method of Bradford (40). Membranes were frozen in liquid nitrogen and stored at −80 °C for future use or immediately used for protein purification.

To extract membrane proteins, membranes were diluted to 5 mg/ml total protein in extraction buffer (20 mM Tris (pH 8), 100 mM NaCl, 3 mM $MgCl_2$, 10 μM GDP, 5 mM β-mercaptoethanol, 2 μg/ml leupeptin, 2 μg/ml aprotinin, 200 μM PMSF, and 1% cholate final). The mixture was stirred on ice for 1 h and then centrifuged at 100,000 × *g* for 45 min. All Ni^{2+} affinity chromatography buffers contained 20 mM NaHEPES (pH 7.5), 100 mM NaCl, 3 mM $MgCl_2$, 2 μg/ml leupeptin, 1 μg/ml aprotinin, 100 μM PMSF, 5 mM β-mercaptoethanol, 10 μM GDP. In addition, buffer N1 contained 0.5% Lubrol; buffer N2 contained 0.5% Lubrol, 500 mM NaCl, and 5 mM imidazole; buffer N3 contained 0.3% cholate; and buffer N4 contained 1% cholate, 30 μM $AlCl_3$, 10 mM $MgCl_2$, and 10 mM NaF.

The membrane protein extract was diluted 5-fold with buffer N1 and mixed with 15 ml of NTA-Ni^{2+}–agarose. The mixture was rotated for 2 h and the NTA-Ni^{2+}–agarose was transferred to a chromatography column. The resin was washed to baseline with buffer N1, N2, and N1, in that order. The resin was rinsed with 15 ml of buffer N3. $G\alpha_q$ was separated from $G\beta_2$-His_6–$G\gamma_2$-$His_{6(8)}$ and eluted using buffer N4 (41).

The eluted $G\alpha_q$ contained phospholipase activity. To remove this contaminant, the pooled fractions were diluted 5-fold in 20 mM MES (pH 6), 1 mM $MgCl_2$, 0.1 mM EDTA, 10 μM GDP, 1 mM DTT, and 0.5% CHAPS and applied to SP-Sepharose in the same buffer. The contaminant was adsorbed to the SP-Sepharose resin. $G\alpha_q$ in the unadsorbed fraction was diluted 4-fold in buffer Q (20 mM Tris (pH 8), 1 mM $MgCl_2$, 0.1 mM EDTA, 10 μM GDP, 1 mM DTT, 0.5% CHAPS) supplemented with 10 mM NaCl and applied to a Source Q column (1 ml) equilibrated with buffer Q. The column was washed to baseline with 10 mM NaCl, and $G\alpha_q$ was eluted over a 40-ml gradient of 10–400 mM NaCl. $G\alpha_q$ eluted between 200 and 250 mM NaCl. $G\alpha_q$ was concentrated in a 10,000 molecular weight cut-off Amicon 0.5-ml centrifugal filter (Millipore). Glycerol was added to 10%, and $G\alpha_q$ was frozen in liquid nitrogen and stored at −80 °C.

To label $G\alpha_q$-E249C, the protein was buffer-exchanged into 20 mM Tris (pH 7.5), 100 mM NaCl, 0.1 mM EDTA, 1 mM $MgCl_2$, 10 μM GDP, 0.5% CHAPS to remove DTT. $G\alpha_q$-E249C (10–20 μM) was incubated with Alexa Fluor 488 C_5 maleimide or Alexa Fluor 594 C_5 maleimide (250 μM) for 1 h on ice. The reaction was quenched by adding 1 mM DTT. Free dye was removed by

successive rounds of buffer exchange into Gα$_q$ storage buffer (20 mM Tris (pH 7.5), 100 mM NaCl, 0.1 mM EDTA, 1 mM $MgCl_2$, 10 μM GDP, 1 mM DTT) without detergent using a 10,000 molecular weight cut-off Amicon 0.5-ml centrifugal filter (Millipore). Fluorescently labeled Gα$_q$-E249C in Gα$_q$ storage buffer supplemented with 0.5% CHAPS was frozen in liquid N_2 and stored at −80 °C. Labeling ratios were determined as described for PLC-β3. Labeling ratios of 2 dye molecules/protein were consistently obtained, suggesting that in addition to Cys^{249}, one of the cysteines at positions 9 and 10 was also labeled.

Wild-type Gα$_q$, Gα$_q$-Cer (38), and Gα$_q$-E249C labeled with Alexa Fluor 488 (Gα$_q$-F) were activated by incubation at 20 °C for 20 h with 1 mM GTPγS in 50 mM NaHEPES (pH 7.5), 100 mM NaCl, 2 mM $MgCl_2$, 1 mM DTT, 200 mM $(NH_4)_2SO_4$, 0.1 mg/ml BSA, and 0.5% CHAPS. The fraction of Gα$_q$ that was activated was determined by [^{35}S]GTPγS binding (16). Fractional activation ranged from 50 to 100% and is accounted for in experiments (see "Results"). Gβ$_1$γ$_2$ was purified after expression with His_6-Gα$_i$ in Sf9 cells as described earlier (41). A human m1AChR construct with an N-terminal FLAG epitope, a C-terminal His_6 tag, and a deletion (residues 232–253) in the third intracellular loop was expressed and purified as described previously (42).

Phospholipid vesicles

Large unilamellar vesicles used in FRET, FCS, and biochemical assays were composed of PE and porcine brain PS (Avanti Polar Lipids). In some FRET and biochemical assays, vesicles also contained porcine brain PIP_2 (Avanti Polar Lipids) and inositol-[2-^{3}H]PIP_2 (PerkinElmer Life Sciences). The phospholipid composition of vesicles used in each experiment is specified in the text. To make vesicles, lipids were dried under argon and resuspended in 50 mM NaHEPES, 100 mM NaCl, 0.2 mM NaEGTA and sonicated to opalescence in a sonication bath. Vesicles were prepared immediately before experiments.

FRET measurements

FRET was used to measure the binding of Gα$_q$ to PLC-β3. Equilibrium FRET measurements were performed using a Fluorolog3-212 spectrophotometer (Horiba Jobin Yvon). For FRET between Alexa Fluor 488- and Alexa Fluor 594-labeled proteins, emission was scanned between 510 and 625 nm following excitation at 475 nm. For FRET measurement between cerulean and Alexa Fluor 594, emission was scanned between 450 and 625 nm following excitation at 410 nm. A 420-nm cut-on filter was placed in-line with the emission path to block scattered excitation light. Excitation and emission bandwidths were 5 nm. Emission scans were obtained with a 1-s integration time in 1- or 2-nm increments.

For equilibrium Gα$_q$–PLC-β3 binding measurements using FRET, fluorescently labeled Gα$_q$ was incubated for 30 min on ice with large unilamellar vesicles (either 0.26 mM PE/PS/PIP_2 (16:4:1) or 0.25 mM PE/PS (4:1)) in binding assay buffer A (50 mM NaHEPES (pH 7.5), 100 mM NaCl, 4 mM $MgCl_2$, 0.2 mM DTT, 0.02% BSA, and 2 mM Ca^{2+}/Na^+ EGTA buffer to achieve a free Ca^{2+} concentration of 60 nM). Following the addition of fluorescently labeled PLC-β3, samples were incubated at 25 °C for 2 min, and immediately thereafter, emission scans were obtained. The assay medium for the FRET measurements is the same as that used in steady-state PLC assays except that PIP_2 and the EGTA/Ca^{2+} buffer were omitted in most binding experiments (see "Results" and Table 1). In some experiments, phospholipid vesicles were omitted entirely or replaced with 0.2% cholate (Table 1).

For equilibrium competitive binding experiments, GTPγS-bound Gα$_q$-E249C labeled with Alexa Fluor 488 (Gα$_q$-F–GTPγS) was incubated with PLC-β3-Q871C labeled with Alexa Fluor 594 (PLC-β3-Q) in the presence of PE/PS (4:1 molar ratio) vesicles in binding assay buffer A for 30 min on ice. Thereafter, unlabeled PLC-β3 was added, samples were incubated at 25 °C for 5 min, and emission scans were obtained.

Binding and competition data were fit as indicated using the Marquardt-Levenberg algorithm in SigmaPlot. For competitive inhibition of binding, IC_{50} values from fits to a single-site competition equation were converted to K_i, the equilibrium K_d for the competing ligand (unlabeled PLC-β3), using the formula, $K_i = IC_{50}/(1 + [Y]/K_{d,Y})$, where Y is ligand whose concentration is held constant (PLC-β3-Q), and $K_{d,Y}$ is its equilibrium dissociation constant for binding to Gα$_q$-F–GTPγS under the same conditions.

FCS measurements

FCS (26) was used to measure both Gα$_q$ binding to PLC-β3 and the binding of Gα$_q$ and PLC-β3 to phospholipid vesicles. FCS measurements were performed using a LSM 880 microscope (Zeiss) equipped with a C-Apochromat ×40, water-immersion objective with a numerical aperture of 1.1 (C-Apochromat ×40/1.1 W Korr, Zeiss). Proteins labeled with Alexa Fluor 488, phospholipid vesicles labeled with $DiOC_{16}$, or free rhodamine 110 (used for calibration) were all excited at 488 nm in number 1.5 coverslip chambers (Lab-Tek, Nalge Nunc). Zen software (Zeiss) was used to obtain time-dependent fluorescence intensities of samples and corresponding autocorrelation curves. The software uses Equation 1 to autocorrelate fluorescence fluctuations.

$$G(\tau) = 1 + \frac{\langle \delta F(t)\delta F(t+\tau)\rangle}{\langle F\rangle^2} \quad \text{(Eq. 1)}$$

In the autocorrelation function $G(\tau)$, fluorescence fluctuations, $\delta F(t)$, defined as the difference between the fluorescence at time t and the time-averaged fluorescence, $\langle F\rangle$, are autocorrelated with fluorescence fluctuations at time $t + \tau$, where τ is the lag time. $G(\tau)$ decays to 1 as τ approaches infinity. Unless otherwise stated, time-dependent fluorescence intensities of a sample were collected over 5 s, 40–50 times in a single experiment. $G(\tau)$ was computed for each 5-s acquisition and averaged over the set of 40–50 acquisitions. To obtain diffusion coefficients, average $G(\tau)$ was fit using Origin to an equation containing one triplet state term and one diffusion term (Equation 2) (43),

$$G(\tau) = 1 + A(1 - F + Fe^{-\tau/\tau_T})\left(\left(1 + \frac{4D\tau}{\omega_o^2}\right)^{-1} \times \left(1 + \frac{4D\tau}{S^2\omega_o^2}\right)^{-1/2}\right) \quad \text{(Eq. 2)}$$

where F is the mean fraction of fluorophores in the triplet state; τ_T is the triplet state lifetime in s; A is the amplitude, which is equal to the inverse of the time-averaged number of molecules

in the detection volume; D is the diffusion coefficient in $\mu m^2/s$; ω_o is the lateral radius of the detection volume in μm; and S is the ratio of the axial to lateral radii ($S = z_o/\omega_o$). Rhodamine 110 was used to determine the dimensions of the FCS detection volume at the beginning of each experiment. FCS curves for rhodamine 110 were fit to Equation 1 using $D = 400$ $\mu m^2/s$ at 22 °C (44), with ω_o, S, τ_T, and F being free parameters. Typical ω_o values were 0.20–0.24 μm, whereas S values ranged from 6 to 10. For rhodamine 110, τ_T, and F were $6.0 \pm 1.7 \times 10^{-6}$ s and 0.14 ± 0.03 ($n = 8$), respectively. S and ω_o were then fixed when FCS data of fluorescently labeled proteins or vesicles were fit to Equation 2, with D, τ_T, and F as free parameters. For GDP- or GTPγS-bound Gα$_q$-F, either alone or in the presence of PLC-β3, τ_T and F were found to be $2.9 \pm 0.8 \times 10^{-5}$ s and 0.23 ± 0.02 ($n = 12$), respectively. For PLC-β3-F, τ_T and F were $4.8 \pm 0.6 \times 10^{-5}$ s and 0.14 ± 0.02 ($n = 3$), respectively. DiO-labeled PE/PS (4:1) vesicles yielded τ_T and F values of $8.4 \pm 0.3 \times 10^{-6}$ s and 0.24 ± 0.05 ($n = 4$), respectively.

To measure equilibrium binding of Gα$_q$ to PLC-β3, FCS curves were obtained for Gα$_q$-F (5–10 nM), bound to either GTPγS or GDP, at different concentrations of unlabeled PLC-β3 in 50 mM NaHEPES (pH 7.5), 100 mM NaCl, 4 mM $MgCl_2$, 0.1 mM DTT, 0.2 mg/ml BSA. The curves were fit to Equation 2 to obtain D, as explained above, for Gα$_q$-F at each unlabeled PLC-β3 concentration. Plots of D *versus* PLC-β3 concentration were fit to a single-site binding equation to obtain K_d. FCS data obtained for Gα$_q$-F and different concentrations of PLC-β3 were also fit to an equation with two diffusion components for free Gα$_q$-F and Gα$_q$-F bound to PLC-β3 (similar to Equation 3). The residuals obtained from the two-component fit were similar to those obtained using Equation 2, and the K_d values did not differ significantly.

To measure the binding of either Gα$_q$-F or PLC-β3–Alx488 (labeled at residue 871) to vesicles, FCS curves of labeled proteins (5–10 nM) were obtained in the presence of PE/PS (4:1) vesicles in 50 mM NaHEPES (pH 7.5), 100 mM NaCl, and 0.2 mM NaEGTA. Ca^{2+} and Mg^{2+} were omitted to minimize vesicle fusion during the experiment. To account for vesicles with multiple bound proteins (45, 46), autocorrelations ($G_m(\tau)$) obtained for a mixture of fluorescent proteins and non-fluorescent vesicles were fit to the following,

$$G_m(\tau) = 1 + A_p(1 - F_p + F_p e^{-\tau/\tau_{T,p}})\left(\left(1 + \frac{4D_p\tau}{\omega_o^2}\right)^{-1} \times \left(1 + \frac{4D_p\tau}{S^2\omega_o^2}\right)^{-1/2}\right) + A_v(1 - F_v + F_v e^{-\tau/\tau_{T,v}}) \times \left(\left(1 + \frac{4D_v\tau}{\omega_o^2}\right)^{-1}\left(1 + \frac{4D_v\tau}{S^2\omega_o^2}\right)^{-1/2}\right) \quad \text{(Eq. 3)}$$

where the parameters are as described above. Parameters with subscript p pertain to free protein in the mixture, and those with subscript v pertain to protein bound to vesicles. In fitting data to Equation 3, F_p, $\tau_{T,p}$, and D_p were fixed at values obtained for labeled protein alone. D_v was fixed at 4.3 μm^2 s^{-1}, the diffusion coefficient of DiO-labeled PE/PS (4:1) vesicles (Fig. 7). Therefore, the only free parameters were A_p, A_v, F_v, and $\tau_{T,v}$. The fraction, f, of protein bound to vesicles was determined using the following equation,

$$f = 1 - \frac{A_p}{A_{p,o}} \quad \text{(Eq. 4)}$$

where $A_{p,o}$ is the amplitude of free labeled protein at the same concentration, with no vesicles.

When D_v was fixed to the diffusion coefficient obtained for DiO-labeled PE/PS (4:1) vesicles, residuals of resulting fits were correlated (see Fig. 7). Better fits were obtained when D_v was allowed to float (Fig. 6). Allowing D_v to float yielded an average value of 6.3 ± 0.7 μm^2 s^{-1}, as opposed to 4.3 μm^2 s^{-1}, for the diffusion coefficient of vesicle-bound Gα$_q$-F and PLC-β3–Alx488. The calculated fractions of Gα$_q$-F and PLC-β3–Alx488 bound to vesicles were similar regardless of whether autocorrelation curves obtained for the two labeled proteins in the presence of vesicles were fit to Equation 3 with D_v as a fixed or free parameter.

Stopped-flow measurements

The kinetics of binding of Gα$_q$-F–GTPγS to PLC-β3-Q was measured by following changes in donor emission using a Bio-Logic SFM-4 stopped-flow fluorometer. Excitation was at 488 nm, and emission was measured at 520 nm. With total flow rates set at 1 ml/s, dead times of 150 ms were achieved. All measurements were performed at 25 °C in binding assay buffer B (50 mM NaHEPES (pH 7.5), 100 mM NaCl, 1 mM $MgCl_2$, 0.2 mM DTT, 0.02% BSA) with PE/PS vesicles. Ca^{2+} was omitted, and Mg^{2+} was reduced compared with binding assay buffer A to reduce vesicle fusion during the course of the measurements.

To measure the association rate, PLC-β3-Q (150, 300, and 450 nM final) was combined with GTPγS-activated Gα$_q$-F (5 or 25 nM final), and the quenching of donor fluorescence was measured for 60 s with a 20-ms integration time. These data were fit to an equation with a single exponent and a linear term to account for photobleaching that is seen with Gα$_q$-F alone,

$$f = f_0 + fe^{-kt} + ct \quad \text{(Eq. 5)}$$

where f_0 is the fluorescence at time 0, f is amplitude associated with rate constant k, and c is the rate of photobleaching. PLC-β3-Q does not alter c.

To measure the dissociation rate, GTPγS-activated Gα$_q$-F (5 or 25 nM) was preincubated with PLC-β3-Q (250 nM final) and PE/PS vesicles in binding assay buffer B. This mixture was combined with an equal volume of wild-type unlabeled PLC-β3 (1800 nM final), and the dequenching of the donor emission was measured for 60 s with a 20-ms integration time. Plots of donor emission *versus* time were initially fit with an equation with either one or two exponential terms,

$$f = f_0 + \sum_{i=1}^{n} f_i(1 - e^{-k_i t}) \quad \text{(Eq. 6)}$$

where f_0 is the fluorescence at time 0 and f_i is the amplitude associated with rate constant k_i. The number of exponential terms is denoted by n. An F-test was performed to determine whether the two fits ($n = 1$ and $n = 2$) were statistically distinguishable (47). We decided that if the equation with fewer

parameters worsened the quality of the fit by $>1\sigma$, the null hypothesis would be rejected. In other words, if the following were true,

$$\frac{\chi^2_{p_1}}{N-p_1} > \frac{\chi^2_{p_2}}{N-p_2} F^{\alpha}_{(N-p_1),(N-p_2)} \quad \text{(Eq. 7)}$$

the equation with more parameters would be a significantly better fit for the data. In the Equation 7, χ^2_{p1} and χ^2_{p2} are the χ^2 goodness-of-fit statistics for fits with one and two exponential terms, respectively. N is the number of analyzed data points, whereas p_1 and p_2 are the number of free parameters associated with fits containing one ($n = 1$) and two ($n = 2$) exponential terms, respectively. The number of free parameters for an equation with n exponential terms, p_n, is $p_n = 2n + 1$. $F^{\alpha}_{(N-p1),(N-p2)}$ is the $(1-\alpha)$ one-sided F statistic with $\alpha = 0.683$ (1σ) and $N-p_1$ and $N-p_2$ degrees of freedom. In these experiments, $N-p_1$ and $N-p_2$ were 2989 and 2987, respectively, yielding an F statistic of 1.02. Fitting the data to Equation 6 with $n = 1$ and $n = 2$ yielded χ^2 statistics that satisfied the expression in Equation 7. Therefore, it was determined that the data were best described by an equation with two exponential terms.

Phospholipase C assay

PLC-β activity was measured by monitoring hydrolysis of [^{3}H]PIP_2 presented in unilamellar vesicles (PE/PS/PIP_2, 16:4:1 molar ratio; 0.25 mM total phospholipid) as described previously (7). PLC-β3 H332A,H379A, a catalytically inactive mutant, was used as a competitive inhibitor of the interaction of wild-type PLC-β3 with $G\alpha_q$–GTPγS (see Fig. 8). To measure the rate of PLC-β deactivation, $G\alpha_q$–GTPγS was incubated with substrate vesicles for 30 min on ice in the presence of 60 nM free Ca^{2+}. The assay was initiated by the addition of PLC-β3, and [^{3}H]IP_3 production was measured at 10-s intervals for 50 s. At that point, 600 μM PLC-β3 H332A,H379A was added, and [^{3}H]IP_3 production was monitored for an additional 4 min. The PLC-β deactivation time, equal to $1/k_{deact}$, is the difference between the time at which PLC-β3 H332A,H379A is added and the time point at which the linear extrapolations of initial and final reaction rates intersect (30).

PLC-β activity was also measured during steady-state receptor signaling using reconstituted vesicles that contained [^{3}H]PIP_2, trimeric G_q, and m1 muscarinic acetylcholine receptor as described by Biddlecome *et al.* (16). To measure the rate of PLC-β deactivation after receptor deactivation in this system, [^{3}H]IP_3 production was measured at 10-s intervals for a total of 40 s to establish a baseline stimulated rate. Atropine and excess GDP were then added to stop receptor signaling, and [^{3}H]IP_3 production was measured for an additional 1–2 min. The PLC-β deactivation time, $1/k_{deact}$, is the difference between the time at which atropine is added and the time at which the linear extrapolations of the pre- and post-atropine reaction rates intersect (16). The fraction of accessible PIP_2 that was hydrolyzed at the time of atropine addition was at most 30%; the decline of the rate did not reflect substrate depletion (7).

Receptor–G_q reconstitution

m1AChR, $G\alpha_q$ variants, and $G\beta_1\gamma_2$ were co-reconstituted in phospholipid vesicles by gel filtration as described previously (16). Briefly, a mixture of phosphatidylethanolamine (1650 μM), phosphatidylserine (980 μM), and cholesteryl hemisuccinate (180 μM) was dried under argon and resuspended in 20 mM NaHEPES (pH 8.0), 100 mM NaCl, 0.4% deoxycholate, and 0.04% cholate. When required, [^{3}H]PIP_2 (100 μM, ~100 cpm/pmol) was included in this mixture. This phospholipid suspension (75 μl) was mixed with m1AChR (13 pmol, 0.087 μM), $G\alpha_q$ variants (80 pmol, 0.53 μM), and Gβγ (120 pmol, 0.80 μM) in 20 mM NaHEPES (pH 7.5), 100 mM NaCl, 3 mM $MgCl_2$, 0.2 mM Na^+/EGTA in a total volume of 150 μl. The mixture was applied to a 6.6 × 250-mm column of Ultrogel AcA34. Protein–phospholipid vesicles were recovered in the void volume. The reconstituted vesicles were stored at 4 °C and used within 48–72 h. Concentration of m1AChR in vesicles was determined by [^{3}H]quinuclidinylbenzilate binding as described previously (16, 48). Total receptor-coupled $G\alpha_q$ was measured by carbachol-stimulated [^{35}S]GTPγS binding as described earlier (48).

Author contributions—P. N. and E. M. R. designed the project and experiments, interpreted data, and prepared the manuscript. P. N. conducted the experiments and analyzed data. A. G. helped plan, analyze, and interpret FCS experiments and data.

Acknowledgments—We thank Ganesh Kadamur, Chad Brautigam, Luke Rice, Suzanne Scarlata, Paul Sternweis, and other colleagues at the University of Texas Southwestern (UTSW) for critical discussion of this work; Jürgen Wess for $G\alpha_q$ C144A,C219A,C330A cDNA; John Sondek for PLC-β3 L859E; Reto Fiolka for the laser used in the stopped-flow experiments; Kate Luby-Phelps and the UTSW Live Cell Imaging Core Laboratory for the FCS facilities; Bree Penninger for help in testing PLC-β dimerization using FRET; and Rolando Valdez and Alexandra Muñiz for technical support.

References

1. Balla, T. (2013) Phosphoinositides: tiny lipids with giant impact on cell regulation. *Physiol. Rev.* **93,** 1019–1137
2. Kadamur, G., and Ross, E. M. (2013) Mammalian phospholipase C. *Annu. Rev. Physiol.* **75,** 127–154
3. Mukhopadhyay, S., and Ross, E. M. (1999) Rapid GTP binding and hydrolysis by G_q promoted by receptor and GTPase-activating proteins. *Proc. Natl. Acad. Sci. U.S.A.* **96,** 9539–9544
4. Lee, C.-W., Lee, K.-H., Lee, S. B., Park, D., and Rhee, S. G. (1994) Regulation of phospholipase C-β4 by ribonucleotides and the α subunit of G_q. *J. Biol. Chem.* **269,** 25335–25338
5. Illenberger, D., Schwald, F., Pimmer, D., Binder, W., Maier, G., Dietrich, A., and Gierschik, P. (1998) Stimulation of phospholipase C-β_2 by the Rho GTPases Cdc42Hs and Rac1. *EMBO J.* **17,** 6241–6249
6. Illenberger, D., Walliser, C., Nurnberg, B., Diaz Lorente, M., and Gierschik, P. (2003) Specificity and structural requirements of phospholipase C-β stimulation by Rho GTPases *versus* G protein βγ dimers. *J. Biol. Chem.* **278,** 3006–3014
7. Philip, F., Kadamur, G., González Silos, R. G., Woodson, J., and Ross, E. M. (2010) Synergistic activation of phospholipase C-β3 by $G\alpha_q$ and Gβγ describes a simple two-state coincidence detector. *Curr. Biol.* **20,** 1327–1335
8. Singer, A. U., Waldo, G. L., Harden, T. K., and Sondek, J. (2002) An unique fold of phospholipase C-β mediates dimerization and interaction with $G\alpha_q$. *Nat. Struct. Biol.* **9,** 32–36

9. Hicks, S. N., Jezyk, M. R., Gershburg, S., Seifert, J. P., Harden, T. K., and Sondek, J. (2008) General and versatile autoinhibition of PLC isozymes. *Mol. Cell* **31,** 383–394
10. Waldo, G. L., Ricks, T. K., Hicks, S. N., Cheever, M. L., Kawano, T., Tsuboi, K., Wang, X., Montell, C., Kozasa, T., Sondek, J., and Harden, T. K. (2010) Kinetic scaffolding mediated by a phospholipase C-β and G_q signaling complex. *Science* **330,** 974–980
11. Lyon, A. M., Tesmer, V. M., Dhamsania, V. D., Thal, D. M., Gutierrez, J., Chowdhury, S., Suddala, K. C., Northup, J. K., and Tesmer, J. J. G. (2011) An autoinhibitory helix in the C-terminal region of phospholipase C-β mediates $G\alpha_q$ activation. *Nat. Struct. Mol. Biol.* **18,** 999–1005
12. Lyon, A. M., Dutta, S., Boguth, C. A., Skiniotis, G., and Tesmer, J. J. G. (2013) Full-length $G\alpha_q$-phospholipase C-β3 structure reveals interfaces of the C-terminal coiled-coil domain. *Nat. Struct. Mol. Biol.* **20,** 355–362
13. Jezyk, M. R., Snyder, J. T., Gershberg, S., Worthylake, D. K., Harden, T. K., and Sondek, J. (2006) Crystal structure of Rac1 bound to its effector phospholipase C-β2. *Nat. Struct. Mol. Biol.* **13,** 1135–1140
14. Paulssen, R. H., Woodson, J., Liu, Z., and Ross, E. M. (1996) Carboxyl-terminal fragments of phospholipase C-β1 with intrinsic G_q GTPase-activating protein (GAP) activity. *J. Biol. Chem.* **271,** 26622–26629
15. Berstein, G., Blank, J. L., Jhon, D.-Y., Exton, J. H., Rhee, S. G., and Ross, E. M. (1992) Phospholipase C-β1 is a GTPase-activating protein for $G_{q/11}$, its physiologic regulator. *Cell* **70,** 411–418
16. Biddlecome, G. H., Berstein, G., and Ross, E. M. (1996) Regulation of phospholipase C-β1 by G_q and m1 muscarinic cholinergic receptor. Steady-state balance of receptor-mediated activation and GTPase-activating protein-promoted deactivation. *J. Biol. Chem.* **271,** 7999–8007
17. Chidiac, P., and Ross, E. M. (1999) PLC-β1 directly accelerates GTP hydrolysis by $G\alpha_q$ and acceleration is inhibited by $G\beta\gamma$ subunits. *J. Biol. Chem.* **274,** 19639–19643
18. Turcotte, M., Tang, W., and Ross, E. M. (2008) Coordinate regulation of G protein signaling via dynamic interactions of receptor and GAP. *PLoS Comput. Biol.* **4,** e1000148
19. Kadamur, G., and Ross, E. M. (2016) Intrinsic pleckstrin homology (PH) domain motion in phospholipase C-β exposes a $G\beta\gamma$ protein binding site. *J. Biol. Chem.* **291,** 11394–11406
20. Ilkaeva, O., Kinch, L. N., Paulssen, R. H., and Ross, E. M. (2002) Mutations of the carboxyl terminal domain of phospholipase C-β1 delineate the dimer interface and a potential $G\alpha_q$ interaction site. *J. Biol. Chem.* **277,** 4294–4300
21. Lyon, A. M., Begley, J. A., Manett, T. D., and Tesmer, J. J. (2014) Molecular mechanisms of phospholipase C-β3 autoinhibition. *Structure* **22,** 1844–1854
22. Charpentier, T. H., Waldo, G. L., Barrett, M. O., Huang, W., Zhang, Q., Harden, T. K., and Sondek, J. (2014) Membrane-induced allosteric control of phospholipase C-β isozymes. *J. Biol. Chem.* **289,** 29545–29557
23. Harden, T. K., Waldo, G. L., Hicks, S. N., and Sondek, J. (2011) Mechanism of activation and inactivation of G_q/phospholipase C-β signaling nodes. *Chem. Rev.* **111,** 6120–6129
24. Segel, I. H. (1975) *Enzyme Kinetics*, pp. 227–273, John Wiley & Sons, Inc., New York
25. Runnels, L. W., and Scarlata, S. F. (1999) Determination of the affinities between heterotrimeric G protein subunits and their phospholipase C-β effectors. *Biochemistry* **38,** 1488–1496
26. Hess, S. T., Huang, S., Heikal, A. A., and Webb, W. W. (2002) Biological and chemical applications of fluorescence correlation spectroscopy: a review. *Biochemistry* **41,** 697–705
27. Magde, D., Elson, E., and Webb, W. W. (1972) Thermodynamic fluctuations in a reacting system: measurement by fluorescence correlation spectroscopy. *Phys. Rev. Lett.* **29,** 705–708
28. Jensen, J. B., Lyssand, J. S., Hague, C., and Hille, B. (2009) Fluorescence changes reveal kinetics steps of muscarinic receptor-mediated modulation of phosphoinositides and Kv7.2/7.7 K^+ channels. *J. Gen. Physiol.* **133,** 347–359
29. Gelb, M. H., Jain, M. K., Hanel, A. M., and Berg, O. G. (1995) Interfacial enzymology of glycerolipid hydrolases: lessons from secreted phospholipases A_2. *Annu. Rev. Biochem.* **64,** 653–688
30. Cassel, D., Levkovitz, H., and Selinger, Z. (1977) The regulatory GTPase cycle of turkey erythrocyte adenylate cyclase. *J. Cyclic Nucleotide Res.* **3,** 393–406
31. Chidiac, P., Markin, V. S., and Ross, E. M. (1999) Kinetic control of guanine nucleotide binding to soluble $G\alpha_q$. *Biochem. Pharmacol.* **58,** 39–48
32. Snyder, J. T., Singer, A. U., Wing, M. R., Harden, T. K., and Sondek, J. (2003) The pleckstrin homology domain of phospholipase C-β2 as an effector site for Rac. *J. Biol. Chem.* **278,** 21099–21104
33. Tsutsumi, R., Fukata, Y., Noritake, J., Iwanaga, T., Perez, F., and Fukata, M. (2009) Identification of G protein α subunit-palmitoylating enzyme. *Mol. Cell Biol.* **29,** 435–447
34. Schaffner, W., and Weissmann, C. (1973) A rapid, sensitive, and specific method for the determination of protein in dilute solution. *Anal. Biochem.* **56,** 502–514
35. Smith, M. R., Liu, Y. L., Matthews, N. T., Rhee, S. G., Sung, W. K., and Kung, H. F. (1994) Phospholipase C-γ1 can induce DNA synthesis by a mechanism independent of its lipase activity. *Proc. Natl. Acad. Sci. U.S.A.* **91,** 6554–6558
36. Hu, J., Wang, Y., Zhang, X., Lloyd, J. R., Li, J. H., Karpiak, J., Costanzi, S., and Wess, J. (2010) Structural basis of G protein-coupled receptor-G protein interactions. *Nat. Chem. Biol.* **6,** 541–548
37. Hepler, J. R., Biddlecome, G. H., Kleuss, C., Camp, L. A., Hofmann, S. L., Ross, E. M., and Gilman, A. G. (1996) Functional importance of the amino terminus of $G_q\alpha$. *J. Biol. Chem.* **271,** 496–504
38. Hughes, T. E., Zhang, H., Logothetis, D. E., and Berlot, C. H. (2001) Visualization of a functional $G\alpha_q$-green fluorescent protein fusion in living cells. *J. Biol. Chem.* **276,** 4227–4235
39. Chan, P., Gabay, M., Wright, F. A., Kan, W., Oner, S. S., Lanier, S. M., Smrcka, A. V., Blumer, J. B., and Tall, G. G. (2011) Purification of heterotrimeric G protein α subunits by GST-Ric-8 association: primary characterization of purified $G\alpha_{olf}$. *J. Biol. Chem.* **286,** 2625–2635
40. Bradford, M. M. (1976) A rapid and sensitive method for the quantitation of microgram quantities of protein utilizing the principle of protein-dye binding. *Anal. Biochem.* **72,** 248–254
41. Kozasa, T., and Gilman, A. G. (1995) Purification of recombinant G proteins from Sf9 cells by hexahistidine tagging of associated subunits: characterization of α_{12} and inhibition of adenylyl cyclase by α_z. *J. Biol. Chem.* **270,** 1734–1741
42. Kruse, A. C., Hu, J., Pan, A. C., Arlow, D. H., Rosenbaum, D. M., Rosemond, E., Green, H. F., Liu, T., Chae, P. S., Dror, R. O., Shaw, D. E., Weis, W. I., Wess, J., and Kobilka, B. K. (2012) Structure and dynamics of the M3 muscarinic acetylcholine receptor. *Nature* **482,** 552–556
43. Widengren, J., and Rigler, R. (1996) Mechanisms of photobleaching investigated by fluorescence correlation spectroscopy. *Bioimaging* **4,** 149–157
44. Gendron, P. O., Avaltroni, F., and Wilkinson, K. J. (2008) Diffusion coefficients of several rhodamine derivatives as determined by pulsed field gradient-nuclear magnetic resonance and fluorescence correlation spectroscopy. *J. Fluoresc.* **18,** 1093–1101
45. Cheng, J., Karri, S., Grauffel, C., Wang, F., Reuter, N., Roberts, M. F., Wintrode, P. L., and Gershenson, A. (2013) Does changing the predicted dynamics of a phospholipase C alter activity and membrane binding? *Biophys. J.* **104,** 185–195
46. Middleton, E. R., and Rhoades, E. (2010) Effects of curvature and composition on α-synuclein binding to lipid vesicles. *Biophys. J.* **99,** 2279–2288
47. Padrick, S. B., and Brautigam, C. A. (2011) Evaluating the stoichiometry of macromolecular complexes using multisignal sedimentation velocity. *Methods* **54,** 39–55
48. Berstein, G., Blank, J. L., Smrcka, A. V., Higashijima, T., Sternweis, P. C., Exton, J. H., and Ross, E. M. (1992) Reconstitution of agonist-stimulated phosphatidylinositol 4,5-bisphosphate hydrolysis using purified m1 muscarinic receptor, $G_{q/11}$, and phospholipase C-β1. *J. Biol. Chem.* **267,** 8081–8088